Available online at www.sciencedirect.com
ScienceDirect
Lithos 97 (2007) 30–57
LITHOS
www.elsevier.com/locate/lithos

The Chimakurti, Errakonda, and Uppalapadu plutons, Eastern Ghats Belt, India: An unusual association of tholeiitic and alkaline magmatism

K. Vijaya Kumar [a,b], Carol D. Frost [a,*], B. Ronald Frost [a], Kevin R. Chamberlain [a]

[a] *Department of Geology and Geophysics, University of Wyoming, Laramie, WY 82071, USA*
[b] *School of Earth Sciences, SRTM University, Nanded-431606, Maharashtra, India*

Received 27 November 2005; accepted 15 November 2006
Available online 12 January 2007

Abstract

Mesoproterozoic tholeiitic and alkalic magmatism is widespread in the southern segment of the Eastern Ghats Belt, India, and is particularly well recorded in three cospatial plutons: Chimakurti, a pluton consisting of clinopyroxenite, anorthosite, and gabbro; Errakonda, a ferrosyenite pluton; and the Uppalapadu nepheline syenite. U–Pb zircon ages of ferrosyenite and nepheline syenite suggest that these cospatial plutons were intruded at approximately 1352 Ma, and Nd and Sr isotope compositions suggest that each pluton experienced varying degrees of crustal assimilation. Petrography, mineral chemistry, geochemistry and isotopic compositions suggest that the clinopyroxenite, anorthosite, and gabbro of the Chimakurti suite were derived from a high-Al tholeiitic parental magma. The ferrosyenite exhibits A-type characteristics and are interpreted as a differentiate or partial melt of a tholeiitic source. The Uppalapadu nepheline syenites were derived from an alkaline (basanitic) parental magma. These three plutons illustrate the spectrum of basaltic magmas that may be involved in producing intraplate intrusive complexes. Tholeiitic magmas emplaced at depth in the crust may differentiate to produce massif anorthosites and related A-type differentiates, represented in the Eastern Ghats Belt by the Chimakurti and Errakonda plutons. More alkalic basalts, such as basanites, will evolve to nepheline syenites like those of the Uppalapadu pluton. The 1352 Ma magmatism in the Eastern Ghats is unusual in that it documents a spatial and temporal association of both tholeiitic and alkaline endmembers of continental rift magmatism.

Keywords: A-type; Alkaline; Tholeiitic; Eastern Ghats Belt; Magmatism; Nd and Sr isotopes; U–Pb geochronology

1. Introduction

Intraplate continental magmatism produces the widest range of magma compositions on Earth. These include mafic–ultramafic layered intrusions, massif anorthosites and their associated ferromonzonites and ferrosyenites, and A-type granites, all considered to be related to a tholeiitic parent, as well as nepheline syenites, derived from an alkaline magma, although these suites seldom occur together. Two different models have been proposed explaining the within-plate cospatial tholeiitic and alkaline magmatism: 1) melts derived from different depths of melting of a homogeneous source (Giret and Lameyre, 1985) and 2) melts derived from heterogeneous sources (Arndt et al., 1998). These two models are based mainly on Phanerozoic associations

* Corresponding author. Tel.: +1 307 766 6254; fax: +1 307 766 6679.
E-mail address: frost@uwyo.edu (C.D. Frost).

0024-4937/$ - see front matter © 2006 Elsevier B.V. All rights reserved.
doi:10.1016/j.lithos.2006.11.008

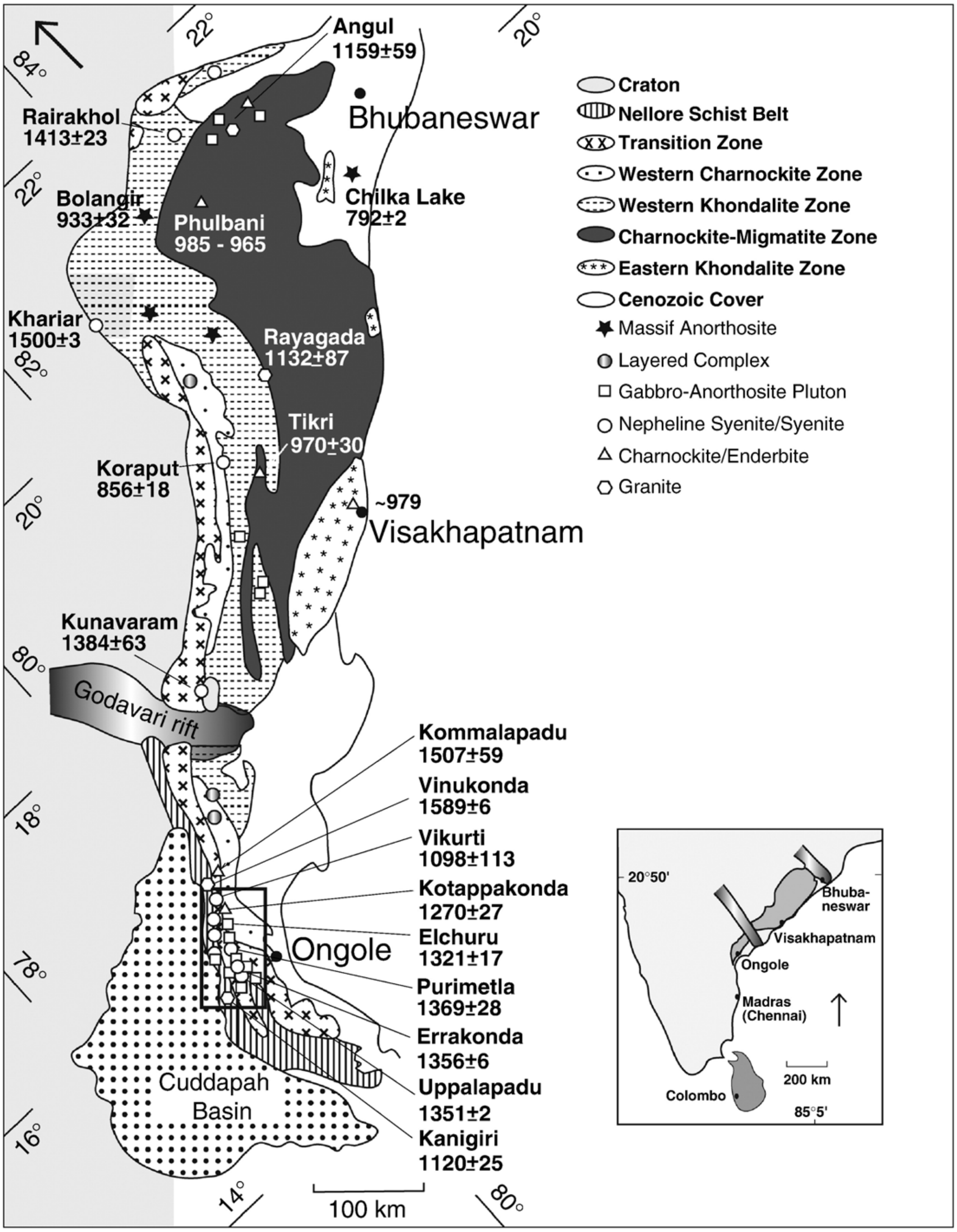

Fig. 1. Simplified geology of Eastern Ghats Belt, India, adapted from Ramakrishnan et al. (1998) and Sarkar and Paul (1998). Note the concentration of Mesoproterozoic igneous activity in the transition and western charnockite zones. The box outlines the Prakasam Province shown in detail in Fig. 2. Sources for age data: Gupta et al. (1984), Grew and Manton (1986), Aftalion et al. (1988), Sarkar et al. (1989), Paul et al. (1990), Shaw et al. (1997), Kovach et al. (1998), Sarkar and Paul (1998), Mezger and Cosca (1999), Aftalion et al. (2000), Krause et al. (2001), Dobmeier et al. (2006), Upadhyay et al. (2006), Upadhyay and Raith (2006) and present study.

and are rarely tested for Precambrian settings (Zozulya et al., 2005). One of the few areas where Precambrian tholeiitic and alkaline magma suites are cospatial is the Chimakurti, Errakonda and Uppalapadu plutons in the Eastern Ghats Belt, India. The Chimakurti mafic–ultramafic pluton is composed of clinopyroxenite, anorthosite, and gabbronorite, and may represent the deeply eroded precursors to the massif anorthosites (cf. Thomas, 1990). The affinity of the Chimakurti pluton to the massif-type anorthosites is exemplified by the presence of high-Al gabbroic and anorthosite dykes, orthopyroxene and clinopyroxene megacrysts (Babu, 1996), and inferred high Al–tholeiite parental liquid composition (see discussion below). Errakonda pluton is composed of ferrosyenite with minor occurrences of ferromonzosyenite and ferrodiorite. The A-type characteristics of the Errakonda pluton include high FeO/(FeO + MgO) ratio, metaluminous character, high K_2O,

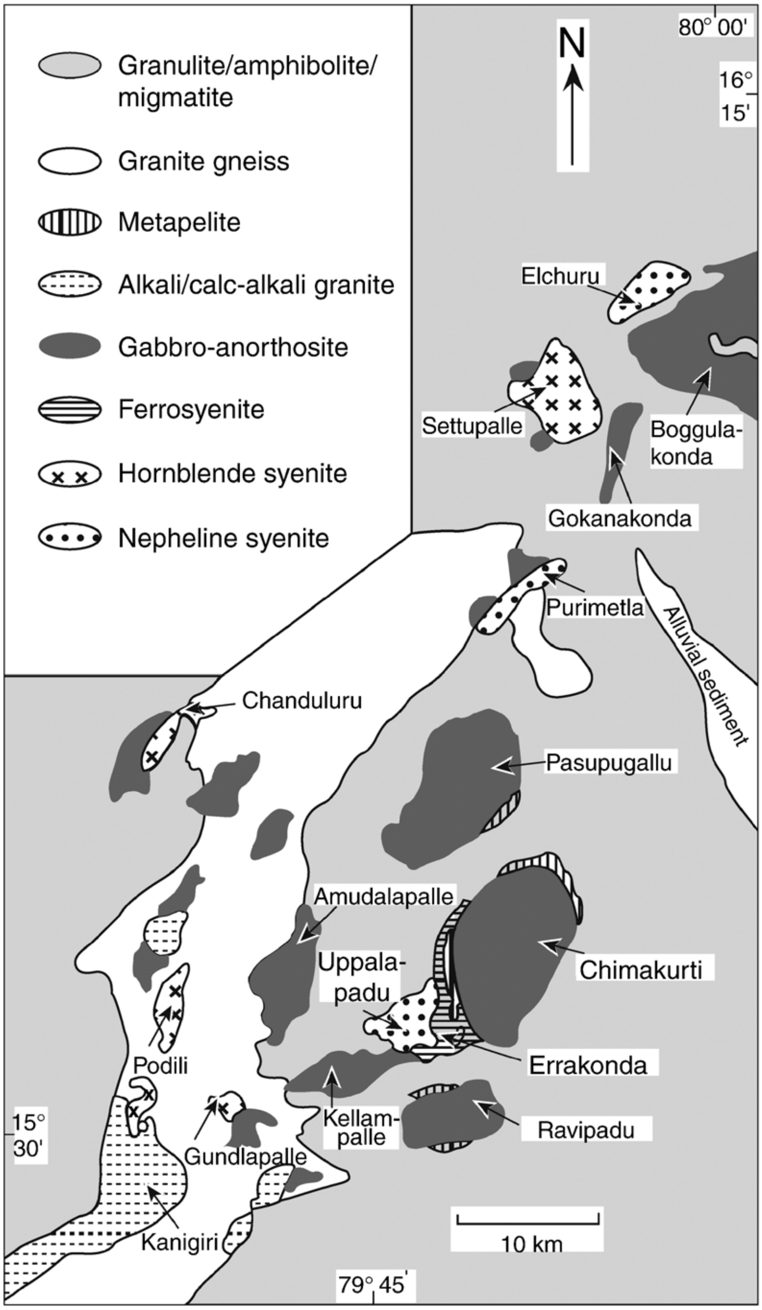

Fig. 2. Simplified geological map showing the distribution of gabbro–anorthosite, syenite (Si-undersaturated and -oversaturated), and granitoid intrusives of the Prakasam Province in the transition zone between the eastern Dharwar craton and the Eastern Ghats Belt (after Rao et al., 1987; Leelanandam, 1989).

molar K/Na ratios, Zr and REE, low CaO and compatible elements, high initial T of crystallization and low f_{O_2}. The Uppalapadu pluton, essentially composed of nepheline syenite, is similar to other Si-undersaturated alkaline plutons in the area, such as Purimetla and Elchuru (Leelanandam, 1989), but lacks mafic rocks.

The goals of the present study are 1) to establish the crystallization ages for this varied magmatic activity, 2) to identify possible parental liquids, 3) to understand the role of crustal contamination in the origin of compositional variations and 4) to develop a model to account for the origin of coeval and cospatial tholeiitic and alkaline magmatism.

2. Regional geology and tectonic setting

The Eastern Ghats Belt (EGB) in Peninsular India (Fig. 1) is a poly-metamorphosed, multi-deformed and

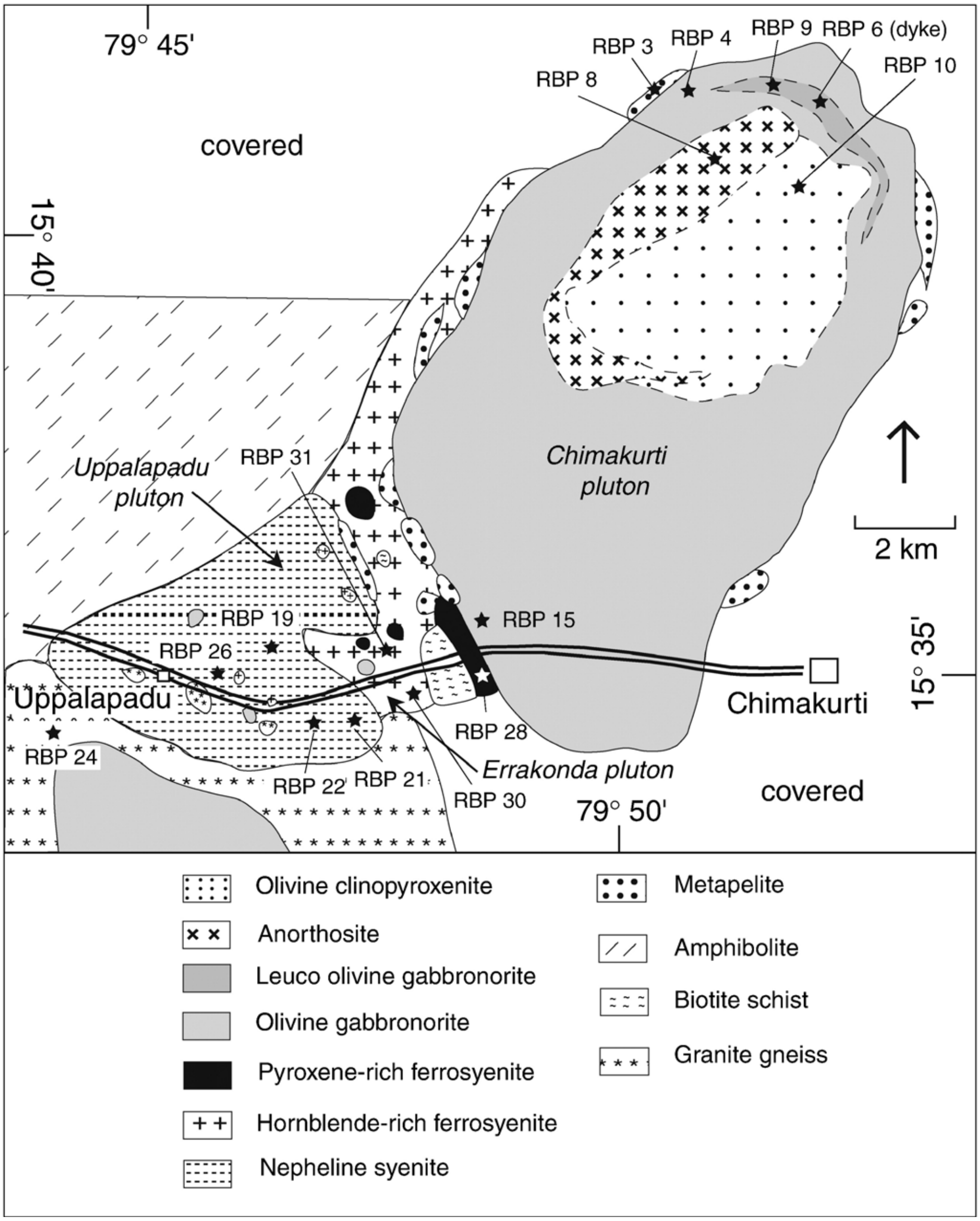

Fig. 3. Geologic map of the Chimakurti–Errakonda–Uppalapadu plutons (modified after Rao et al., 1987; Krishna Reddy et al., 1998). Stars give the locations of samples analyzed in this study.

deeply eroded granulite terrain. The EGB is segmented into four, northeast–southwest trending longitudinal zones; from northwest to southeast they include 1) western charnockite zone, 2) western khondalite zone, 3) charnockite–migmatite zone and 4) eastern khondalite zone (Ramakrishnan et al., 1998; Fig. 1). The boundary between the Archean craton and Proterozoic mobile belt is marked by a transition zone, which contains intermingled cratonic amphibolites/granite gneisses and mobile belt granulites. In addition the EGB is separated into northern and southern segments by the Godavari rift.

Based on a recent synthesis of the geological and isotopic data, Dobmeier and Raith (2003) have proposed a subdivision of the EGB into four crustal provinces each of which has different geological histories. These four provinces are further divided into a number of domains based on lithology, structure and metamorphic grade (see Fig. 2 of Dobmeier and Raith, 2003). The present study area falls within the Ongole domain of the Krishna Province of Dobmeier and Raith (2003). The Ongole domain consists of granulite facies rocks, which, based upon Nd model ages, are considered to be metasediments that were derived from the eastern Dharwar cratonic granitoids. The domain has experienced a short-lived mantle-derived magmatism between 1.72 and 1.70 Ma followed by a prolonged polyphase granulite facies metamorphism between 1.65 and 1.55 Ma (Mezger and Cosca, 1999; Kovach et al., 2001). Dobmeier and Raith (2003) correlated the 1.75–1.55 event in Ongole domain to collision between eastern Dharwar craton with the Napier complex of East Antarctica. A second major igneous event, associated with extensive tholeiitic and alkaline magmatism (the Prakasam Alkaline Province; Fig. 2) occurred in the Ongole domain between 1.4 and 1.2 Ma (Fig. 1), possibly in response to continental rifting and/or post-collisional relaxation of the thickened lithosphere (Leelanandam, 1989; Ratnakar and Leelanandam, 1989; Vijaya Kumar and Ratnakar, 2001; Dobmeier and Raith, 2003; Upadhyay et al., 2006). The Prakasam Alkaline Province (PAP) is one of the few places in the world where there is a close spatial association of gabbro-anorthosite, ferrosyenite and nepheline syenite (Rao et al., 1987; Leelanandam, 1989; Fig. 2).

3. Geology of the Chimakurti, Errakonda and Uppalapadu plutons

Rocks of the Chimakurti and Errakonda plutons are exposed on undulating hills, where they have been extensively quarried, whereas the nepheline syenites of the Uppalapadu pluton are mostly restricted to ground-level exposures in barren fields, dried-up ponds and road cuts. The three plutons intruded country rock in the transition zone between granulite facies and amphibolite facies rocks (Fig. 3).

The Chimakurti pluton is an elliptical body occupying an area of ~90 km^2. In map view the Chimakurti pluton appears concentrically zoned, with a sequence from core to margin of 1) olivine clinopyroxenite, 2) anorthosite, 3) olivine gabbronorite and 4) gabbronorite (Fig. 3). Field and petrologic and geochemical relations (Rao et al., 1987; Leelanandam, 1993a, 1994) suggest that erosion exposes a section through the Chimakurti magma chamber. The central clinopyroxenite may represent the early cumulates forming the base of the magma chamber, whereas the gabbronorites occupy the upper levels of chamber. At the contact with the Chimakurti pluton, metapelitic rocks record imprints of ultrahigh temperature contact metamorphism (>1000 °C) at mid-crustal conditions (~6–7 kb) (Babu, 1996; Dasgupta et al., 1997). Two-pyroxene thermometry records temperatures of ~1100 °C at the centre of the Chimakurti pluton (Rao et al., 1998).

The clinopyroxenite, anorthosite, and gabbro portions of the Chimakurti pluton show gradational relationships in terms of color index and grain size in the field. Clinopyroxenite and anorthosite are coarse-grained (grain size up to 4 cm). There is a gradual decrease in the grain size from core to the periphery of the pluton (3–4 cm to <1 mm). Peripheral gabbronorite, especially in the southwestern margin, shows well-developed magmatic layering with inward dips of moderate to steep angles (72° to 78°; Babu, 1996). Some of the marginal gabbronorites are very fine-grained ($\ll$1 mm) and may represent chilled liquids. Locally, some of the marginal rocks show effects of strain including bending of plagioclase. High-Al gabbroic dykes are most common in the inner portions of the Chimakurti pluton. A rare hercynite adcumulate band of 50 m length with a uniform thickness of 4 cm is reported within the leucogabbronorite from the Chimakurti pluton (Babu et al., 1997).

Ferrosyenites of Errakonda occur along the western and southwestern margin of the Chimakurti pluton. They are separated in places from the Chimakurti pluton by metapelites and magnetite–quartzites (Fig. 3). The ferrosyenites contain abundant enclaves and xenoliths of both the country rock and of gabbronorite. The ferrosyenites share sharp contact with both the Chimakurti gabbros and Uppalapadu nepheline syenites. The ferrosyenites include both hornblende-rich, pyroxene-poor varieties and clinopyroxene-rich ones. The hornblende-rich ones are more abundant and display layering

Table 1
U–Pb zircon data for ferrosyenite and nepheline syenite from the Errakonda–Uppalapadu plutons

Sample no.	Sample name	Weight (mg)	U (ppm)	Pb (ppm)	Com Pb [a] (ppm)	Corrected atomic ratios							$^{206}Pb/^{238}U$ age (Ma)	$^{207}Pb/^{235}U$ age (Ma)	$^{207}Pb/^{206}Pb$ age (Ma)	±	*Rho* [b]	% Disc. [c]
						$^{206}Pb/^{204}Pb$ [d] (corr.)	$^{206}Pb/^{238}U$ [e, f] (rad.)	%err	$^{207}Pb/^{235}U$ [e, f] (rad.)	%err	$^{207}Pb/^{206}Pb$ [e, f] (rad.)	%err						
RBP 28 ferrosyenite						1351.5±2 Ma MSWD=0.85 (4-point chord)												
1	m1 (5; *d* −1°)	0.130	567	138.32	1.10	7086	0.2299	0.42	2.7461	0.42	0.0866	0.04	1334	1341	1352.0	±0.87	0.99	1.46
2	aa3 (3; *d* −1°)	0.010	549	139.52	6.54	1164	0.2283	0.32	2.7251	0.33	0.0866	0.08	1325	1335	1351.2	±1.50	0.97	2.11
3	aa1 (4; *d* −1°)	0.009	535	135.83	6.52	1157	0.2323	0.32	2.7729	0.33	0.0866	0.08	1347	1348	1351.0	±1.60	0.97	0.37
4	aa4 (1; *d* −1°)	0.002	496	133.96	10.47	671	0.2312	0.42	2.7613	0.49	0.0866	0.29	1341	1345	1352.1	±5.30	0.81	0.93
5	aa5 (2; *d* −1°)	0.003	808	207.57	3.55	3185	0.2322	0.34	2.7785	0.35	0.0868	0.12	1346	1350	1355.6	±2.30	0.94	0.77
RBP 21 nepheline syenite						1356.5±6.5 Ma MSWD=5.4 (4-point chord)												
6	aa1 (1; *d* −3°)	0.053	100	24.14	0.12	11047	0.2309	0.32	2.7601	0.33	0.0867	0.07	1339	1345	1353.5	±1.30	0.98	1.16
7	aa2 (2; *d* −3°)	0.115	107	25.43	0.04	36418	0.2299	0.32	2.7497	0.32	0.0868	0.05	1334	1342	1355.1	±0.90	0.99	1.74
8	ua1 (5; *d* −3°)	0.232	75	17.56	0.29	3370	0.2201	0.38	2.6249	0.39	0.0865	0.05	1282	1308	1349.6	±0.96	0.99	5.49
9	ua2 (41; *d* −3°)	0.820	142	34.04	0.26	7301	0.2218	0.38	2.6453	0.39	0.0865	0.04	1292	1313	1349.1	±0.82	0.99	4.71
10	aa3 (1; *d* −3°)	0.010	193	44.38	3.24	738	0.2056	0.38	2.4534	0.42	0.0865	0.16	1205	1258	1350.3	±3.20	0.91	11.77
11	aa4 (3; *d* −3°)	0.009	125	33.74	2.38	734	0.2308	0.76	2.7736	0.81	0.0872	0.26	1339	1348	1364.2	±5.10	0.94	2.07
12	aa6 (4; *d* −3°)	0.007	107	39.83	11.63	145	0.2375	0.45	2.8633	0.74	0.0874	0.55	1374	1372	1370.4	±11.00	0.61	−1.35

Zircon fraction: *d*° represent angles of diamagnetic susceptibility on a barrier style Frantz separator; aa=air-abraded. Number of grains and diamagnetic angles are given in parentheses.

[a] Common Pb (ppm) corrected for laboratory blank.

[b] $^{206}Pb/^{238}U$ vs. $^{207}Pb/^{235}U$ error correlation coefficient.

[c] Percent discordance.

[d] Ratio corrected for blank and mass discrimination.

[e] Radiogenic Pb in ratios; all values corrected for blank and mass discrimination.

[f] %Err are 2σ in percent.

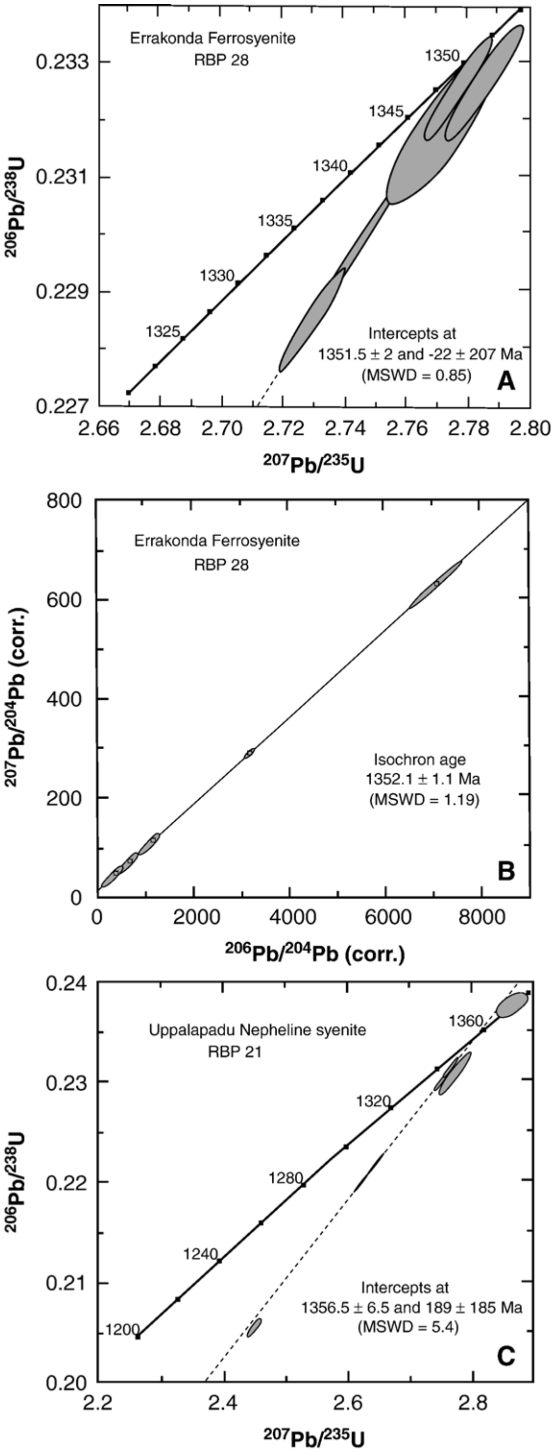

Fig. 4. (A) U–Pb concordia diagram for zircons from ferrosyenite (RBP 28), (B) Pb–Pb isochron for zircons from ferrosyenite, (C) concordia diagram for zircons from nepheline syenite (RBP 21).

of hornblende-rich and feldspar-rich bands along the margins, whereas the pyroxene-rich varieties are massive. Locally, ferrosyenites grade into monzodiorite and ferrodiorite.

The Uppalapadu nepheline syenite, which occupies an area of ~30 km^2, intrudes the southern margin of the Errakonda pluton (Fig. 3). The nepheline syenite is massive and pegmatitic. It is relatively more deformed than the Chimakurti and Errakonda plutons, containing well-defined foliation along the margins and in local shear zones (Krishna Reddy et al., 1998). The Uppalapadu nepheline syenite contains abundant xenoliths of country rock as well as of gabbro and hornblende-rich ferrosyenite indicating that structurally high levels of the pluton are exposed. Gabbroic and syenitic xenoliths in the nepheline syenite are texturally and mineralogically similar to the gabbronorite and ferrosyenite of the Chimakurti and Errakonda plutons, respectively. The Chimakurti, Errakonda, and Uppalapadu plutons appear to be contemporaneous based upon the occurrence of gabbro xenoliths within ferrosyenite and nepheline syenite, nepheline syenite dykes in gabbro–anorthosites, and noritic gabbro and gabbro dykes in nepheline syenites.

4. Analytical procedures

Zircon dissolution and chemistry were adapted from methods developed by Krogh (1973) and Parrish (1987). Aliquots of dissolved sample were spiked with a mixed ^{208}Pb/^{235}U tracer. Pb and U samples were loaded onto single rhenium filaments with silica gel and graphite, respectively; isotopic compositions were measured in multi-collector, static mode on a VG Sector mass spectrometer at the University of Wyoming. Mass discrimination factors of 0.06±0.04%/amu for Pb and 0.0±0.06%/amu for U were determined by replicate analyses of NIST SRM 981 and U-500, respectively. Procedural blank was 10 pg Pb or less over the course of the study. U blanks were consistently less than 1 pg. Concordia coordinates, intercepts, and uncertainties were calculated using PBDAT and ISOPLOT programs (Ludwig, 1988, 1991); initial Pb isotopic compositions were based on measured Pb isotopic compositions of coexisting feldspars. The decay constants used by PBDAT are those recommended by the I.U.G.S. Subcommission on Geochronology (Steiger and Jäger, 1977): 0.155125×10^{-9}/yr for ^{238}U, 0.98485×10^{-9}/yr for ^{235}U and present-day ^{238}U/^{235}U = 137.88.

Mineral compositions were determined on the JEOL 8900 Superprobe at the University of Wyoming using 15 kV voltage and sample current 20 nA for biotites and

Table 2
Petrographic summary of cumulate rocks from the Chimakurti pluton

Rock type	Texture	Cumulus phases	Intercumulus phases	Coronal minerals
Olivine clinopyroxenite	Adcumulate	Cpx+Ol±Opx	Opx+Pl	Opx+Amph Symp+Spl
Anorthosite	Adcumulate	Pl±Ol	Opx+Ol+Cpx+Mag+Ilm	Opx+Amph Symp+Spl
Olivine gabbronorite	Mesocumulate	Pl+Ol+Cpx+Opx	Opx+Pl+Ol+Cpx+Mag+Ilm	Opx+Amph Symp+Spl+Bt
Gabbronorite	Orthocumulate	Pl+Opx+Cpx	Opx+Pl+Cpx+Mag+Ilm	Opx+Amph Symp+Spl+Bt

10 nA for feldspars. Analyses were corrected using the ZAF procedure. Abundances of major elements and, Ba, Nb, Rb, Sr, and Zr were determined by XRF at XRAL Laboratories, Don Mills, Ontario, Canada. Abundances of the REEs, Th, Y, and U were determined by ICP–MS at XRAL. Detection limits for major elements are 0.01%; replicate analyses are within 1%. Detection limits are 2 ppm for Rb, Nb, V, and Pb; 1 ppm for Ba, Cr, Co and Ni; 0.5 ppm for Sr, Y, Zr, Sc, Cu and Zn; and 0.1 ppm for Th, U and REE except Eu, Ho and Lu for which the detection limit is 0.05 ppm.

For isotopic analyses 80 to 100 mg of sample were dissolved in HF-HNO_3. After conversion to chlorides, one-third of the sample was combined with mixed ^{87}Rb–^{84}Sr, and ^{149}Sm–^{146}Nd spikes. Rb, Sr, and REE were separated by conventional cation-exchange procedures. Sm and Nd were further separated in di-ethylhexyl orthophosphoric acid columns. All isotopic measurements were made on a VG Sector multi-collector mass spectrometer at the University of Wyoming. An average $^{87}Sr/^{86}Sr$ isotopic ratio of 0.710267±6 (2 S.E.M.) was measured for NBS987 Sr and an average $^{143}Nd/^{144}Nd$ ratio of 0.511856±7 (2 S.E.M.) normalized to $^{146}Nd/^{144}Nd=0.7219$ was measured for the La Jolla standard. Uncertainties in Sr isotopic measurements are ±0.00002 and uncertainties in Nd

Table 3
Representative biotite compositions from the nepheline syenite of Uppalapadu

Sample	RBP 19	RBP 19	RBP 19	RBP 19	RBP 19	RBP 19	RBP 26	RBP 26	RBP 26	RBP 26
Spot no.	1	2	3	4	5	6	7	8	9	10
SiO_2	31.73	31.99	32.02	31.98	31.99	31.98	30.59	31.65	31.29	30.99
TiO_2	0.82	0.89	0.65	0.69	0.72	0.77	0.04	0.04	0.25	0.23
Al_2O_3	19.94	19.88	19.99	20.00	19.75	19.71	25.19	25.97	25.41	25.21
Fe_2O_3 [a]	5.28	3.34	3.50	4.20	5.52	5.44	0.92	0.00	0.00	0.35
FeO	26.95	28.95	29.14	28.94	28.17	27.76	30.16	30.16	29.89	29.73
MnO	0.21	0.24	0.24	0.25	0.23	0.26	0.35	0.31	0.46	0.52
MgO	3.72	2.74	2.63	2.62	2.76	2.89	0.66	0.62	0.96	1.01
CaO	0.13	0.01	0.00	0.00	0.17	0.12	0.02	0.00	0.00	0.03
Na_2O	0.08	0.11	0.10	0.12	0.15	0.14	0.12	0.10	0.08	0.16
K_2O	7.33	9.42	9.58	9.47	8.32	8.36	9.48	9.70	9.69	9.28
Total	96.20	97.58	97.86	98.28	97.79	97.44	97.54	98.56	98.04	97.51
Cation proportions calculated on the basis of 22 oxygens										
Si	5.020	5.069	5.068	5.041	5.038	5.046	4.825	4.905	4.884	4.863
Ti	0.098	0.106	0.077	0.082	0.085	0.091	0.005	0.005	0.029	0.027
Al	3.718	3.712	3.729	3.715	3.665	3.665	4.682	4.743	4.674	4.662
Fe^{3+}	0.629	0.398	0.417	0.498	0.654	0.646	0.109	0.000	0.000	0.041
Fe^{2+}	3.565	3.835	3.856	3.815	3.709	3.662	3.977	3.908	3.901	3.901
Mn	0.028	0.032	0.032	0.033	0.031	0.035	0.047	0.041	0.061	0.069
Mg	0.877	0.647	0.621	0.616	0.648	0.680	0.155	0.143	0.223	0.236
Ca	0.022	0.002	0.000	0.000	0.029	0.020	0.003	0.000	0.000	0.005
Na	0.025	0.034	0.031	0.037	0.046	0.043	0.037	0.030	0.024	0.049
K	1.479	1.904	1.934	1.904	1.671	1.683	1.907	1.918	1.929	1.858
X_{Mg}	0.173	0.133	0.127	0.125	0.129	0.136	0.037	0.035	0.054	0.057

Spot nos. 1 and 2 are big euhedral grains associated with pyrite–pyrrhotite; 3 and 4 are small euhedral inclusions within nepheline; 5 and 6 are acicular biotites warping around nepheline crystals; 7 and 8 small inclusions in nepheline; 9 and 10 are small irregular grains associated with hercynite and corundum.

$X_{Mg}=Mg/(Mg+Fe^T)$.

[a] Fe_2O_3 is calculated using charge balance.

Table 4
Representative feldspar and nepheline compositions from the nepheline syenite of Uppalapadu

Sample	RBP 19	RBP 26	RBP 19	RBP 19	RBP 19	RBP 26	RBP 26		RBP 26	RBP 26	RBP 19	RBP 19	RBP 19
	Matrix	Albite in	Re-integrated	Re-integrated	Re-integrated	Re-integrated	Re-integrated						
	Albite	Nepheline	Feldspar	Feldspar	Feldspar	Feldspar	Feldspar		Nepheline	Nepheline	Nepheline	Nepheline	Nepheline
SiO_2	68.24	66.69	65.78	66.33	65.20	66.24	66.87		43.56	42.88	42.78	41.96	43.31
Al_2O_3	19.05	20.18	18.70	19.08	18.90	20.08	19.78		33.91	34.29	34.54	34.89	33.68
Fe_2O_3	0.03	0.03	0.03	0.01	0.02	0.10	0.01		0.10	0.05	0.02	0.23	0.00
CaO	0.07	0.21	0.00	0.00	0.01	1.16	0.49		0.26	0.24	0.19	0.01	0.01
Na_2O	12.25	11.94	5.12	7.31	3.95	9.87	9.79		16.79	16.80	16.72	17.04	16.98
K_2O	0.07	0.04	9.85	6.86	11.59	1.79	2.65		5.75	6.02	6.43	6.59	6.71
Total	99.71	99.09	99.48	99.58	99.66	99.24	99.58		100.37	100.29	100.68	100.72	100.69
Cation proportions calculated on the basis of 8 oxygens													
Si	2.996	2.949	2.991	2.984	2.979	2.944	2.965		2.082	2.056	2.047	2.015	2.076
Al	0.986	1.052	1.003	1.011	1.019	1.052	1.034		1.910	1.938	1.948	1.975	1.903
Fe	0.001	0.001	0.001	0.000	0.001	0.004	0.000		0.003	0.002	0.001	0.008	0.000
Ca	0.003	0.010	0.000	0.000	0.000	0.055	0.023		0.014	0.013	0.010	0.000	0.001
Na	1.043	1.024	0.439	0.624	0.341	0.848	0.835		1.556	1.562	1.551	1.586	1.578
K	0.004	0.002	0.584	0.406	0.684	0.105	0.157		0.351	0.368	0.392	0.404	0.410
Total	5.033	5.038	5.019	5.025	5.024	5.007	5.014		5.915	5.939	5.950	5.989	5.967
Ab	0.993	0.988	0.429	0.606	0.333	0.841	0.823	Ne	77.778	77.790	76.877	77.532	77.561
An	0.003	0.010	0.000	0.000	0.000	0.055	0.023	Ks	19.568	20.438	21.653	22.098	22.439
Or	0.004	0.002	0.571	0.394	0.667	0.104	0.155	Qtz	2.654	1.772	1.470	0.370	0.000

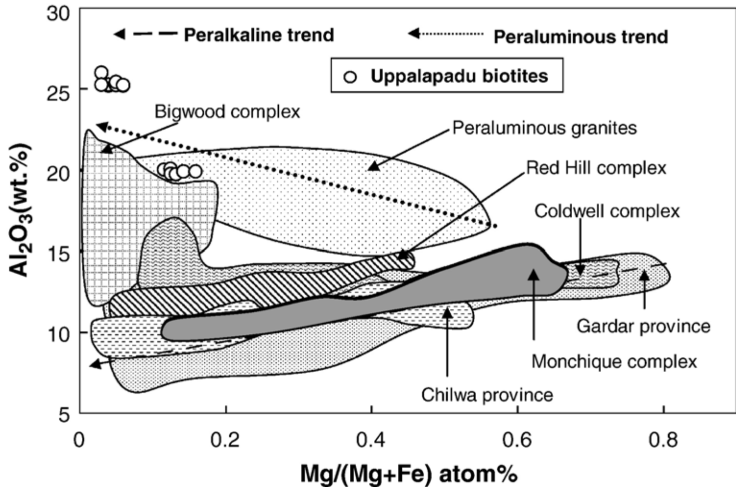

Fig. 5. Mg/(Mg+Fe) vs. Al_2O_3 variation in biotites of Uppalapadu nepheline syenites. Biotite compositional fields for other nepheline syenites (and related rocks) and peraluminous granites are plotted for comparison. Sources of data for nepheline syenites and related rocks: Duke and Edgar (1977), Powell (1978), Rock (1978), Mitchell and Platt (1982), Woolley and Platt (1986), Henderson et al. (1989) and Finch et al. (1995); for peraluminous granites: De Albuquerque (1973), Joyce (1973), Harris (1974), Guidotti et al. (1975), Phillips et al. (1981) and Speer (1981).

measurements are ±0.00001 (2 S.E.M.). Blanks are 50 pg for Rb, Sr, Nd, Sm, and no blank correction was made. Uncertainties in Rb, Sr, Nd and Sm concentrations on replicate dissolutions are ±2% of the measured value; uncertainties on initial ε_{Nd} are ±0.5 epsilon units.

5. Geochronology: the timing of magmatism

We have selected two samples, a ferrosyenite and a nepheline syenite, for U–Pb geochronology to date the timing of the Errakonda and Uppalapadu plutons, respectively. We infer from field relations that the age of Errakonda pluton will also indicate the emplacement age of the Chimakurti pluton. We analyzed five fractions of zircon, including 4 air-abraded fractions, from the ferrosyenite sample and seven fractions, including 4 air-abraded fractions, from the nepheline syenite. Most of the analyzed fractions were composed of between one and five grains (Table 1). Optically visible cores were not present in either ferrosyenite or nepheline syenite zircons.

5.1. Ferrosyenite (RBP 28) of Errakonda

Zircons from the ferrosyenite (RBP 28) are colorless to light yellowish green. They are from 40 μm to 300 μm in length, and most of them are euhedral, doubly terminated crystals. Igneous zoning is locally present. Irregular to radial fractures are observed rarely in few zircon grains. A few grains contain colorless centers but honey colored rims. Some of the zoned crystals display radiation damage but none are metamict. Zircons

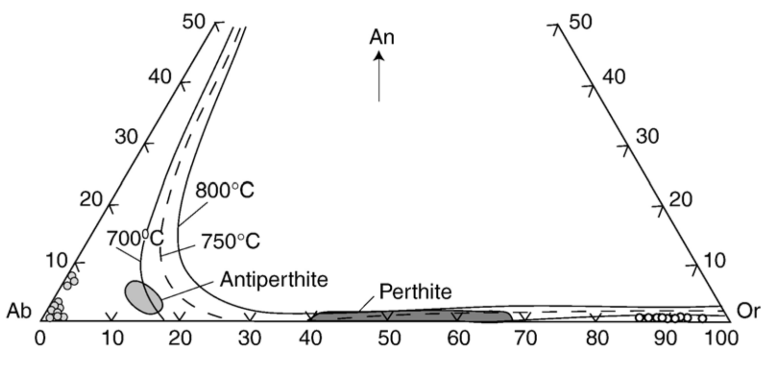

Fig. 6. Compositions of re-integrated alkali feldspars from Uppalapadu nepheline syenites in a portion of Ab–Or–An system. Isotherms are after Elkins and Grove (1990).

selected for U–Pb analysis were clear without any fractures or inclusions.

U and Pb concentrations in ferrosyenite zircons are uniform (496–567 and 134–139 ppm, respectively) except for one fraction (aa5), which has higher 808 ppm U and 208 ppm Pb (Table 1). Concordia coordinates were calculated using Pb isotopic compositions of co-existing feldspar as an estimate for initial Pb isotopic compositions of zircon. Feldspar grains were dissolved in steps (e.g. Chamberlain and Bowring, 2001) and the least radiogenic values were 16.436±0.013, 15.586±0.018, 36.204±0.058 for $^{206}Pb/^{204}Pb$, $^{207}Pb/^{204}Pb$ and $^{208}Pb/^{204}Pb$, respectively. On a conventional concordia diagram (Fig. 4A) the zircon data plot in a nearly concordant cluster; discordance ranges from 0.37% to 2.11%. Four of the points plot in a linear array with a narrow range of $^{207}Pb/^{206}Pb$ ages from 1351 to 1352 Ma, the fifth point (aa5) plots to the right with a $^{207}Pb/^{206}Pb$ age of 1356 Ma. A four-point linear regression without aa5 yields an upper intercept age of 1352±2 Ma (MSWD=0.85) that we interpret as the age of crystallization. In this model, the grains in fraction aa5 are interpreted to include a slight amount of older, inherited zircon. On a Pb–Pb isochron diagram (Fig. 4B) all the fractions of RBP 28 zircons, including aa5, define a linear trend and yield an identical age (1352±1 Ma; MSWD=1.19) suggesting that the Pb loss is recent and that the scatter on the concordia diagram may be due to our choice of initial Pb isotopic composition rather than inheritance. Based on the agreement of Pb–Pb and U–Pb regressions and near concordance of the zircon data, we interpret 1352±2 Ma as the crystallization age for the ferrosyenite.

5.2. Nepheline syenite (RBP 21) of Uppalapadu

Zircons of nepheline syenite (RBP 21) are sub- to anhedral, do not exhibit strong zonation, and are texturally distinct from those of the ferrosyenite. Some of the zircons have equidimensional platy shapes, and are texturally associated with titanite in thin section. The zircon yield in the nepheline syenite was less than that from the ferrosyenite.

U and Pb concentrations in the nepheline syenite zircons (75–193 and 18–44 ppm, respectively) are fivefold lower than those of ferrosyenite zircons (Table 1). Feldspar Pb isotopic compositions from this sample were measured as 15.908±0.013, 15.368±0.018, 35.967±0.057 for $^{206}Pb/^{204}Pb$, $^{207}Pb/^{204}Pb$ and $^{208}Pb/^{204}Pb$, respectively, and used as estimates of initial Pb isotopic composition in zircon. On a concordia plot (Fig. 4C), the data form a non-linear array with a wide

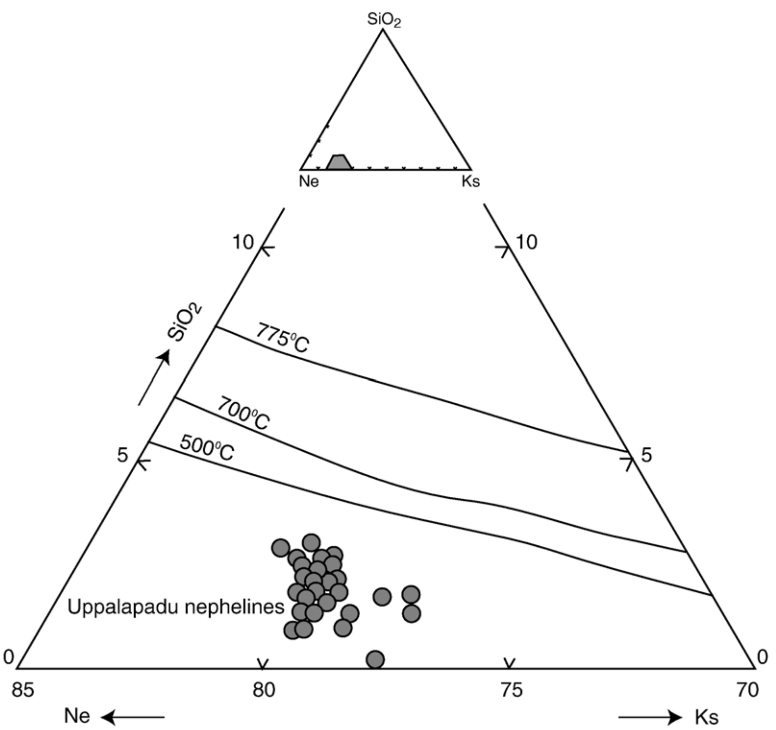

Fig. 7. A portion of Ne–Ks–Si system showing the projected compositions of Uppalapadu nephelines. Isotherms are after Hamilton (1961).

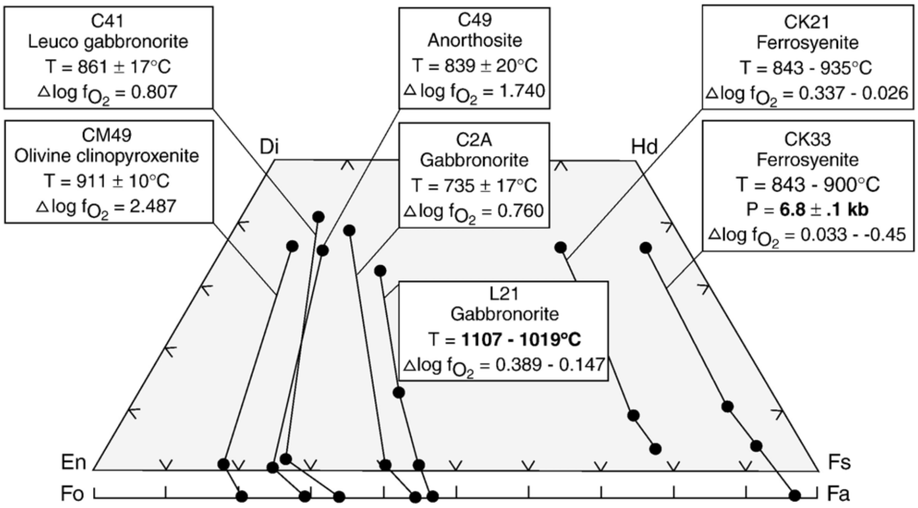

Fig. 8. Pyroxene quadrilateral and Fo–Fa join showing the compositions of pyroxenes and olivine (data from Leelanandam, 1993a, 1994; Babu, 1996) from mafic rocks and ferrosyenite of Chimakurti pluton. Intrinsic parameters are calculated using the QUILF program of Andersen et al. (1993). $\Delta f(O_2)$ is the difference in $\log f(O_2)$ between sample and that of FMQ buffer at a given temperature.

range of discordance (−1.3 to 12%) and $^{207}Pb/^{206}Pb$ ages (1349 to 1370 Ma). The scatter cannot be attributed entirely to choice of initial Pb isotopic composition as data from both the fractions with the highest $^{206}Pb/^{204}Pb$ (# 7, 36418) and one of the lowest (# 11, 734) yield $^{207}Pb/^{206}Pb$ ages that are older than fractions with intermediate $^{206}Pb/^{204}Pb$ (# 6, 8, 9). Consequently, some of the scatter is interpreted to reflect inheritance of older zircon components. Our best estimate for the crystallization age of this rock comes from a linear regression of the 4 analyses with least discordant data and youngest Pb/Pb ages (# 6, 9; Table 1), which yielded 1356±7 Ma (MSWD=5.6). The scatter in this regression (MSWD=5.6) is interpreted to reflect slight amounts of inheritance in the analyzed grains, so this intercept date is a maximum age. The youngest $^{207}Pb/^{206}Pb$ age of the least discordant point (1353±1; # 6, 1.2% discordant) can also be interpreted as a maximum age. Field relations require the nepheline syenite to be coeval to or slightly younger than the ferrosyenite. Therefore we interpret 1352 Ma as the maximum crystallization age of the Chimakurti, Errakonda and Uppalapadu plutons.

6. Petrography

6.1. Chimakurti pluton

The Chimakurti pluton consists of clinopyroxenite, anorthosite, and gabbro, which are cumulates of Cpx+Ol, Pl+Ol, and Pl+Opx+Cpx±Ol, respectively, with variable amounts of intercumulus phases. A petrographic summary of mafic cumulate rocks is given in Table 2. Based on field and petrography observations the following variations from center to the western and southwestern margins of the Chimakurti pluton are noted: 1) general decrease in grain size, 2) systematic decrease and final disappearance of modal olivine and gradual increase in modal orthopyroxene, magnetite, ilmenite and secondary amphibole and biotite, 3) increase in zoning and clouding of plagioclase, 4) variation in the cumulus state from ad- to meso- to ortho-cumulate, 5) increase of textural anisotropy as indicated by layering and oriented plagioclase, and 6) grading of marginal gabbronorites into norites with a concomitant increase in modal plagioclase. The high-Al gabbroic dykes are mineralogically similar to the olivine gabbronorites (Table 2) but are texturally distinct. They exhibit fine- to medium-grained equigranular to sub-ophitic textures. Coronal assemblages and secondary minerals are absent. Plagioclase comprises more than 50% of the rock and clinopyroxene is more abundant than orthopyroxene.

6.2. Errakonda pluton

The rocks of the Errakonda pluton are medium-grained and exhibit hypidiomorphic textures; local megacrysts of amphibole and perthite are present. The alkali feldspar is mostly mesoperthite but independent grains of K-feldspar and albite are present in a few samples. The type and

Table 5
Major element compositions and CIPW norms of the rocks from Chimakurti–Errakonda–Uppalapadu plutons

Sample	RBP 10	RBP 8	RBP 9	RBP 15	RBP 6	C4 [a]	AMP1 [a]
Rock type	Olivine clinopyroxenite	Anorthosite	Olivine gabbronorite	Gabbronorite	High-Al gabbroic dyke	Marginal gabbro	Ferrosyenite
Pluton	C	C	C	C	C	C	E
SiO_2	47.40	50.70	50.90	52.20	49.60	49.14	50.90
TiO_2	0.31	0.12	0.25	0.38	0.39	0.85	1.67
Al_2O_3	6.26	27.70	17.30	16.40	15.80	15.21	16.80
Fe_2O_3	10.30	1.97	5.92	8.68	9.74	3.01	1.77
FeO						10.66	8.79
MnO	0.14	0.02	0.09	0.14	0.14	0.19	0.20
MgO	22.60	2.46	10.40	9.55	9.24	8.12	3.11
CaO	11.80	13.30	12.70	10.30	12.10	9.75	7.30
Na_2O	0.54	3.10	2.17	2.39	2.33	2.14	4.30
K_2O	0.15	0.30	0.24	0.29	0.28	0.23	2.88
P_2O_5	0.02	0.02	0.02	0.02	0.02	0.10	0.63
LOI	0.10	0.35	0.10	0.00	0.30		
Total	99.62	100.04	100.09	100.35	99.94	99.40	98.35
Fe*	0.29	0.42	0.34	0.45	0.49	0.62	0.77
q							
or	0.89	1.77	1.42	1.71	1.65	1.36	17.32
ab	4.65	26.32	18.45	20.31	19.97	18.19	31.23
an	14.41	61.09	36.96	33.28	32.21	31.43	18.33
ne							3.11
c							
di	35.62	4.07	20.97	14.44	23.05	13.63	12.01
hy	12.16	4.64	12.78	27.28	9.18	27.45	
ol	29.36	1.38	7.61	0.30	11.00	1.69	10.66
mt	2.28	0.43	1.29	1.90	2.15	4.39	2.61
il	0.59	0.23	0.47	0.72	0.74	1.63	3.23
ap	0.05	0.05	0.05	0.05	0.05	0.23	1.48

$Fe^* = FeO^t/(FeO^t + MgO)$. [a]Data from Babu (1996).

modal proportions of mafic mineral vary widely. Hornblende–syenites are most common with lesser amounts of clinopyroxene–syenite. Other phases include fayalite, Fe–Ti oxides, zircon, apatite and quartz. Primary biotite is absent. Primary amphibole (ferropargasite; Babu, 1996) is subhedral and contains inclusions of clinopyroxene. Orthopyroxene occurs locally, mostly associated with clinopyroxene. Some samples of the ferrosyenite contain inverted pigeonite (Babu and Leelanandam, 1993; Leelanandam, 1993a, 1994) suggesting a high initial crystallization temperature. A few olivine grains (Fo_3–Fo_1) are in textural equilibrium with quartz. Some samples contain garnet occurring along the interfaces between plagioclase and pyroxenes, olivine and Fe–Ti oxides (Leelanandam, 1993b), which is interpreted as a subsolidus phase. The assemblage of Fa–Opx–Aug–Qtz–Grt–Ilm (+Amp+Inverted Pig) is encountered in a single sample (CK-33). Ferrodiorite (e.g. AMP1 in Table 5) contains plagioclase and amphibole with minor clinopyroxene. Among the accessory phases, zircon shows spectacular zoning and is more abundant in the hornblende-rich varieties. Apatite occurs as inclusions in mafic minerals and as interstitial grains.

6.3. Uppalapadu pluton

The nepheline syenite of the Uppalapadu pluton displays equigranular hypidiomorphic, porphyritic and pegmatitic textures. The rock contains perthite and nepheline as essential minerals. Both subsolvus and hypersolvus alkali feldspars are found; in the former, sodic plagioclase show conspicuous zoning. Nepheline occurs as coarse subhedral grains containing inclusions of feldspars and microlites of biotite. Biotite is the sole mafic phase and makes up less than 5% of the mode. Accessory and secondary minerals include Fe sulfides, magnetite, zircon, titanate, apatite, calcite, cancrinite, allanite, garnet, corundum and hercynite. Locally acicular biotite and

FSA2[a]	RBP 30	RBP 28	RBP 31	RBP 22	RBP 21	RBP 24	RBP 3
Ferrosyenite	Ferrosyenite	Ferrosyenite	Ferrosyenite	Nepheline syenite	Nepheline syenite	Granite gneiss	Metapelite
E	E	E	E	U	U	Country rock	Country rock
55.92	61.50	67.00	71.20	58.40	58.10	77.00	48.00
1.66	0.74	0.27	0.20	0.20	0.02	0.09	1.47
17.58	15.80	16.00	14.20	20.80	22.60	12.30	25.10
1.29	7.55	4.00	3.12	4.62	3.90	1.44	16.10
5.96							
0.15	0.16	0.10	0.07	0.09	0.04	0.02	0.24
1.59	0.78	0.05	0.04	0.50	0.01	0.00	4.45
3.92	3.22	1.59	1.27	2.08	0.74	0.63	1.70
3.88	4.71	4.91	4.59	6.18	8.61	3.80	1.53
6.08	5.24	5.92	5.03	5.79	5.30	4.41	1.69
0.66	0.22	0.02	0.06	0.14	0.04	0.06	0.05
	0.01	0.25	0.40	1.40	0.80	0.25	0.00
98.69	99.93	100.11	100.18	100.20	100.16	100.00	100.33
0.82	0.90	0.99	0.99	0.89	1.00	1.00	0.78
	4.40	10.99	21.60			36.20	14.12
36.40	31.20	35.16	29.34	34.75	31.62	26.18	10.11
33.25	40.11	41.72	39.01	41.09	40.78	32.24	13.12
12.76	6.57	4.17	3.33	9.55	3.46	2.73	8.21
				6.53	17.74		
				0.94	1.47	0.29	17.95
2.16	6.99	3.23	2.34				
3.86	7.15	3.30	2.68			1.75	30.02
4.91				5.41	3.94		
1.90	1.65	0.87	0.68	1.01	0.86	0.32	3.54
3.19	1.42	0.51	0.38	0.38	0.04	0.17	2.83
1.55	0.51	0.05	0.14	0.32	0.09	0.14	0.12

magnetite warp around nepheline crystals. Corundum and hercynite are closely associated with biotite.

7. Mineral chemistry and crystallization conditions

In this paper we summarize available data from the rocks of the Chimakurti and Errakonda plutons (Leelanandam, 1993a, 1994; Babu, 1996) and present new mineral analyses from the nepheline syenites of Uppalapadu (Tables 3 and 4).

7.1. Mineral chemistry of the Chimakurti and Errakonda plutons

Olivine compositions in the Chimakurti mafic cumulates ranges from Fo_{83} to Fo_{66}, orthopyroxene from $Mg\#_{82}$ to $Mg\#_{55}$, and clinopyroxene from $Mg\#_{94}$ to $Mg\#_{68}$. Plagioclase composition ranges from An_{70} to An_{46}. In the Errakonda ferrosyenites the olivine composition ranges from Fo_{3} to Fo_{1}, orthopyroxene from $Mg\#_{26}$ to $Mg\#_{7}$, and clinopyroxene from $Mg\#_{40}$ to $Mg\#_{12}$. Plagioclase ranges from An_{65} to An_{3}.

7.2. Mineral chemistry of the Uppalapadu pluton

7.2.1. Biotite

The biotites of Uppalapadu are iron-rich and are the most aluminous known (Al_2O_3 = 19.7 to 26 wt.%; Table 3) (Fig. 5). Biotite with highest Al_2O_3 coexists with corundum and hercynite. The solution of Al_2O_3 into biotite can be modeled by the following equilibrium:

$$\underset{\text{magnetite}}{Fe_3O_4} + \underset{\text{in melt}}{3SiO_2} + \underset{\text{Ts-component in biotite}}{3Al_2Si_{-1}Fe_{-1}} = \underset{\text{corundum}}{3Al_2O_3} + \underset{\text{melt}}{0.5O_2} + \text{Annite component}$$

This equilibrium indicates that high Al content in biotite is favored by rocks with a high oxygen fugacity, high Al_2O_3 activity, and low SiO_2 activity. The Uppalapadu pluton is one of the few nepheline syenites that are corundum-bearing; the high-Al_2O_3 and low-SiO_2 activities of these rocks explain why they contain the most Al-rich biotite found in nature.

7.2.2. Alkali feldspars

Individual feldspars are completely re-equilibrated and show near end member compositions (Fig. 6). The original composition of the feldspars was estimated by determining the relative abundances of two feldspars in the perthite and antiperthite in backscattered electron images. These reintegrated compositions were used to calculate crystallization temperatures. The original composition of the feldspars ranges from $Ab_{84}Or_{10}An_6$ to $Ab_{33}Or_{67}An_0$ (Table 4). These compositions would be in equilibrium at temperatures 700 to 800 °C (Fig. 6).

7.2.3. Nepheline

The nepheline compositions fall in the range of Ne_{76-79} Ks_{19-22} Qtz_{0-3} with negligible quantities of Fe nepheline (0.00–0.28) and anorthite component (0.05–1.38) (Table 4). The Uppalapadu nephelines are similar to the nephelines from Elchuru pluton to the north of Uppalapadu (Upadhyay et al., 2006). The low Si solid solution (calculated on molar basis) in the Uppalapadu nephelines (Fig. 7) suggests re-equilibration.

7.3. Pressure estimates

The emplacement pressure for the Errakonda pluton can be estimated from the Fs–Fa–Pig–Hd–Qtz assemblage (ferrosyenite sample CK33 of Leelanandam, 1993a, 1994) using the QUILF program of Andersen et al. (1993). The uncertainties in pressure and temperature calculations given in Fig. 8 refer to the precision of the mathematical fits; the accuracy of the estimates are hard to assess but are probably on the order of 0.5 kb for pressure and ±25 °C for temperature (see Frost et al., 2000). Calculated pressure is 6.8 kb, corresponding to a depth of ~20 km (Fig. 8). The pressure obtained here is similar to the pressure estimate of 6–7 kb based on thermally metamorphosed pelitic rock in the contact aureole (Babu, 1996; Dasgupta et al., 1997). Evidence for high-pressure crystallization of the Chimakurti pluton also comes from the presence of abundant clinopyroxene cumulates. Experimental work on dry basaltic magmas indicates that at high pressures clinopyroxene will crystallize prior to plagioclase (Green and Ringwood, 1967; Elthon and Scarfe, 1984).

7.4. Temperature estimates

The crystallization temperature for the marginal gabbronorite of the Chimakurti pluton (L21; Babu, 1996) was greater than 1100 °C, based on the composition of inverted pigeonite (Fig. 8). Relict pigeonite in the ferrosyenite records a minimum *T* of >900 °C. This high temperature of emplacement is consistent with the partial melting of metapelitic enclaves. The two-pyroxene temperatures range from 911 to 735 °C (Fig. 8). This temperature range records different stages at which intercrystalline Fe–Mg–Ca exchange was locked in during cooling.

Using the nepheline–alkali feldspar thermometry of Powell and Powell (1977) we calculate a crystallization temperature of 800±70 °C for the Uppalapadu nepheline syenite, which is somewhat higher than the results of feldspar thermometry of 715 °C (Elkins and Grove, 1990; Fig. 6). This discrepancy is probably caused by subsolidus reequilibration of the feldspars.

7.5. Oxygen fugacity

Oxygen fugacity was calculated using the QUILF program of Andersen et al. (1993), on the assemblages Ol–Opx–Aug–Mag–Ilm in the Chimakurti pluton and Ol–Pgt–Qtz–Mag–Ilm in the ferrosyenite. The gabbro and anorthosite members of the Chimakurti pluton crystallized at oxygen fugacities ranging 2.48 to 0.39 log units above FMQ, with f_{O_2} falling with increasing X_{Fe} (Fig. 8). The ferrosyenites crystallized at $\Delta\log(f_{O_2})=-0.03$ to -0.45. This f_{O_2} trend reflects the iron-enrichment associated with differentiation, which is typical of evolution of tholeiitic magma by fractional crystallization (Frost and Lindsley, 1992).

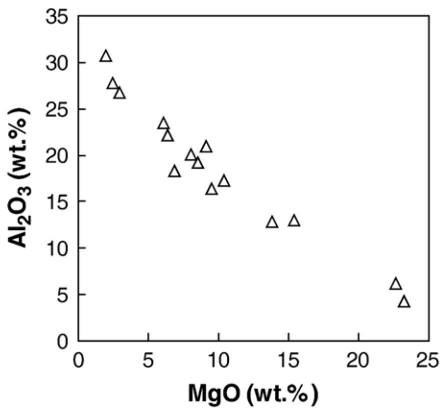

Fig. 9. MgO vs. Al_2O_3 variation diagram for the cumulate rocks of the Chimakurti pluton. For discussion, see the text.

Table 6
Trace and rare earth element compositions of the rocks from the Chimakurti–Errakonda–Uppalapadu plutons

Sample	RBP 10	RBP 8	RBP 9	RBP 15	RBP 6	C4 [a]	AMP1 [a]	FSA2 [a]	RBP 30	RBP 28	RBP 31	RBP 22	RBP 21	RBP 24	RBP 3
Rock type	Olivine clinopyroxenite	Anorthosite	Olivine gabbronorite	Gabbronorite	High-Al gabbroic dyke	Marginal gabbro	Ferrosyenite	Ferrosyenite	Ferrosyenite	Ferrosyenite	Ferrosyenite	Nepheline syenite	Nepheline syenite	Granite gneiss	Metapelite
Pluton	C	C	C	C	C	C	E	E	E	E	E	U	U	Country rock	Country rock
Sc	44	4	22	28	36	37	20	8	10	2	0	1			23
Cr	1360	23	228	62	136	127	33		13	18	30	11	8	24	137
V	190	28	112	114	164	228	112	9	30	2	3	11		2	160
Co	87	11	33	42	47				13	2	2	4		1	40
Ni	990	54	188	111	127	97	19	2	4	3	3	7		3	90
Cu	285	27	55	53	64	74	39	11	17	7	3	13	9	4	39
Zn	55	15	34	57	47	106	145	76	132	67	60	53	37	36	54
Rb	5	3		6	5	1	142	140	133	124	21	111	123	125	30
Sr	198	886	540	540	648	167	766	527	167	32	47	176	31	11	173
Y	8	7	6	8	9	20	31	26	58	32	54	18	13	61	30
Zr	30	9	15	15	19	41	135	93	739	892	516	442	347	240	264
Nb	2	2				2	56	78	94	71	94	48	36	83	15
Ba	112	258	194	181	273	78	2095	2659	845	207	400	460	138	64	1110
Th	1	1	1	1	1	2	8	3	25	36		3	1	29	
U									4	4		1	0	6	
Mo	2	4	3	2	2				5	8	3	1	3	4	1
Li	3	2	1	2	1				13	5	5	35	15	3	8
REE															
La	2.8	3.1	3.1	2.0	3.8	7.0	69.8	94.4	214.0	364.0		80.3	30.6	9.7	
Ce	6.7	5.3	6.6	4.1	8.3	14.0	131.7	181.4	391.0	639.0		123.0	30.7	19.6	
Pr	1.0	0.7	0.9	0.6	1.5	2.0	14.6	20.8	41.3	62.8		11.4	2.2	2.7	
Nd	4.5	2.1	3.7	2.6	5.8	10.0	52.6	75.7	132.0	186.0		33.1	5.5	12.6	
Sm	1.2	0.4	1.0	0.8	1.7	2.0	9.2	12.8	20.7	22.7		4.5	0.6	6.4	
Eu	0.5	0.5	0.6	0.6	1.1	1.0	3.9	3.2	2.2	1.1		1.1	0.4	0.1	
Gd	1.3	0.4	1.1	0.9	1.8	3.0	8.6	11.8	16.6	14.6		3.4	0.5	9.7	
Tb	0.2		0.2	0.2	0.4	1.0	1.1	1.8	2.6	1.9		0.5		2.0	
Dy	1.2	0.3	1.0	1.0	1.6	3.0	6.3	9.5	12.9	7.8		0.5	0.3	12.6	
Ho	0.2	0.1	0.2	0.2	0.4	1.0	1.1	1.9	2.7	1.5		0.6	0.1	2.7	
Er	0.6	0.2	0.5	0.6	0.9	2.0	3.1	5.2	7.3	4.0		1.5	0.2	7.1	
Yb	0.5	0.2	0.5	0.5	0.7	2.0	2.8	4.7	7.0	4.4		1.6	0.3	5.1	
Lu	0.1		0.1	0.1	0.1		0.5	0.7	1.1	0.8		0.3		0.7	
∑REE	20.8	13.3	19.5	14.2	28.1	48.0	305.3	423.7	851.4	1310.6		261.8	71.4	91.1	

[a] Data from Babu (1996).

8. Geochemistry

8.1. Major elements

The hypersthene normative nature of the mafic rocks of the Chimakurti attests to their tholeiitic nature (Table 5). Compositions of the cumulate rocks of the Chimakurti pluton are dependent more on the abundance of cumulate minerals than on differentiation (Fig. 9). There is an inverse relationship between the abundances of Al_2O_3 and MgO, with the Al_2O_3 end of the trend represented by anorthosites and MgO end represented by clinopyroxenites. Trace element compositions also corroborate their cumulus nature (Table 6). In view of the cumulus nature of the Chimakurti samples they are not plotted in the major and trace element variation diagrams. Both the Errakonda and Uppalapadu plutons contain ferroan, alkalic rocks, but the Uppalapadu intrusion is Si-undersaturated and the more extremely alkalic of the two (Table 5; Fig. 10A and B). Trace element composition of both ferrosyenite and nepheline syenite are consistent with their origin as within-plate granitoids (Fig. 10C and D). We have plotted the major elements from the Errakonda–Uppalapadu plutons on variation diagrams that use FeO^t (wt.%) as a monitor of differentiation (Fig. 11) i.e., decreasing FeO^t with increasing differentiation. The Errakonda ferrosyenites contain higher SiO_2, TiO_2, CaO and lower Al_2O_3, Na_2O and K_2O than the Uppalapadu nepheline syenites (Fig. 11; Table 5) for similar FeO^t contents. The liquid lines of descent for Al_2O_3, Na_2O and K_2O are distinctly different for ferrosyenites and nepheline syenites.

8.2. Trace elements

Concentrations of Rb, Zr, Y and Nb (Table 6) are variable for similar FeO^t contents in the ferrosyenites and nepheline syenites. Y shows a gradual increase but Rb

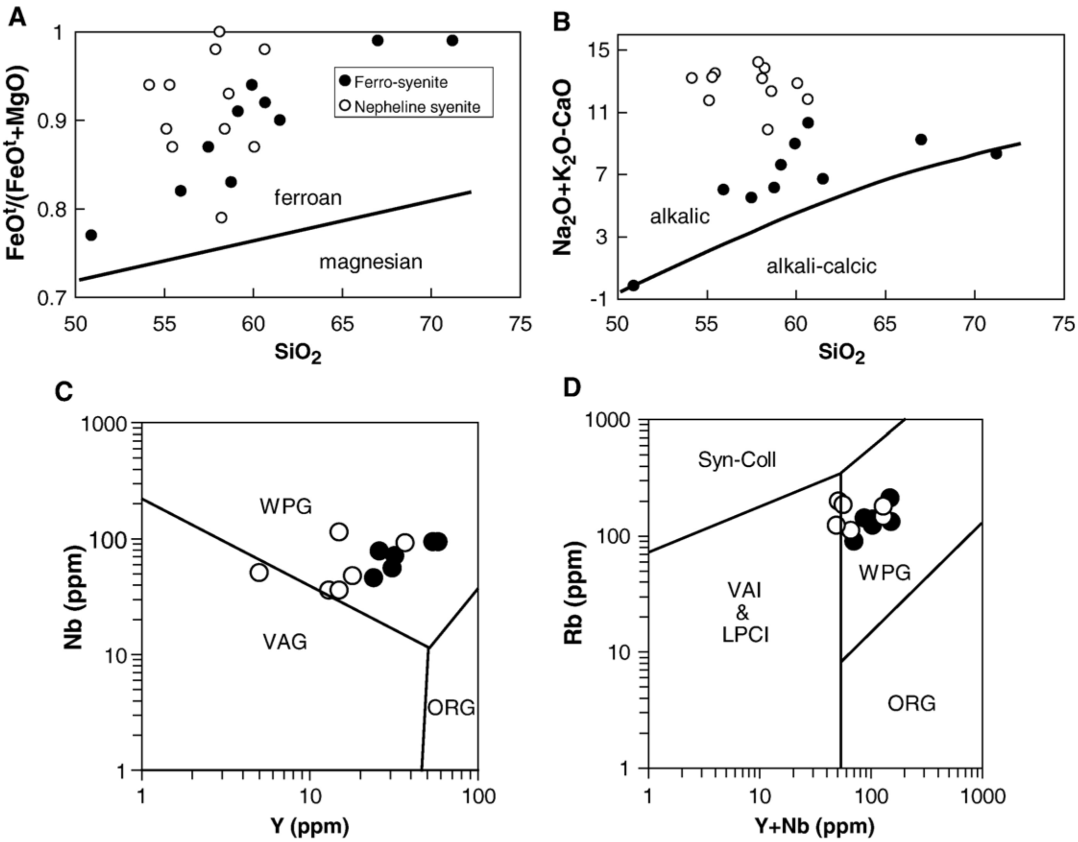

Fig. 10. Plot of $FeO^t/(FeO^t+MgO)$ versus SiO_2 (A); plot of Na_2O+K_2O–CaO versus SiO_2 (B). Both ferrosyenite and nepheline syenite lie in alkalic and ferroan fields. Alkalic–alkali–calcic, and ferroan–magnesian boundaries from B.R. Frost et al. (2001a). Nb vs. Y and Rb vs. Y+Nb plots (C) and (D) show ferrosyenite and nepheline syenite within the within-plate granites. ORG=oceanic ridge granites; VAG=volcanic arc granites; Syn-Coll=syn-collision granites; WPG=within-plate granites. Fields from Pearce et al. (1984). Sources of data: Bhattacharyya et al. (1981), Rao et al. (1987), Czygan and Goldenberg (1989), Babu (1996) and Krishna Reddy et al. (1998).

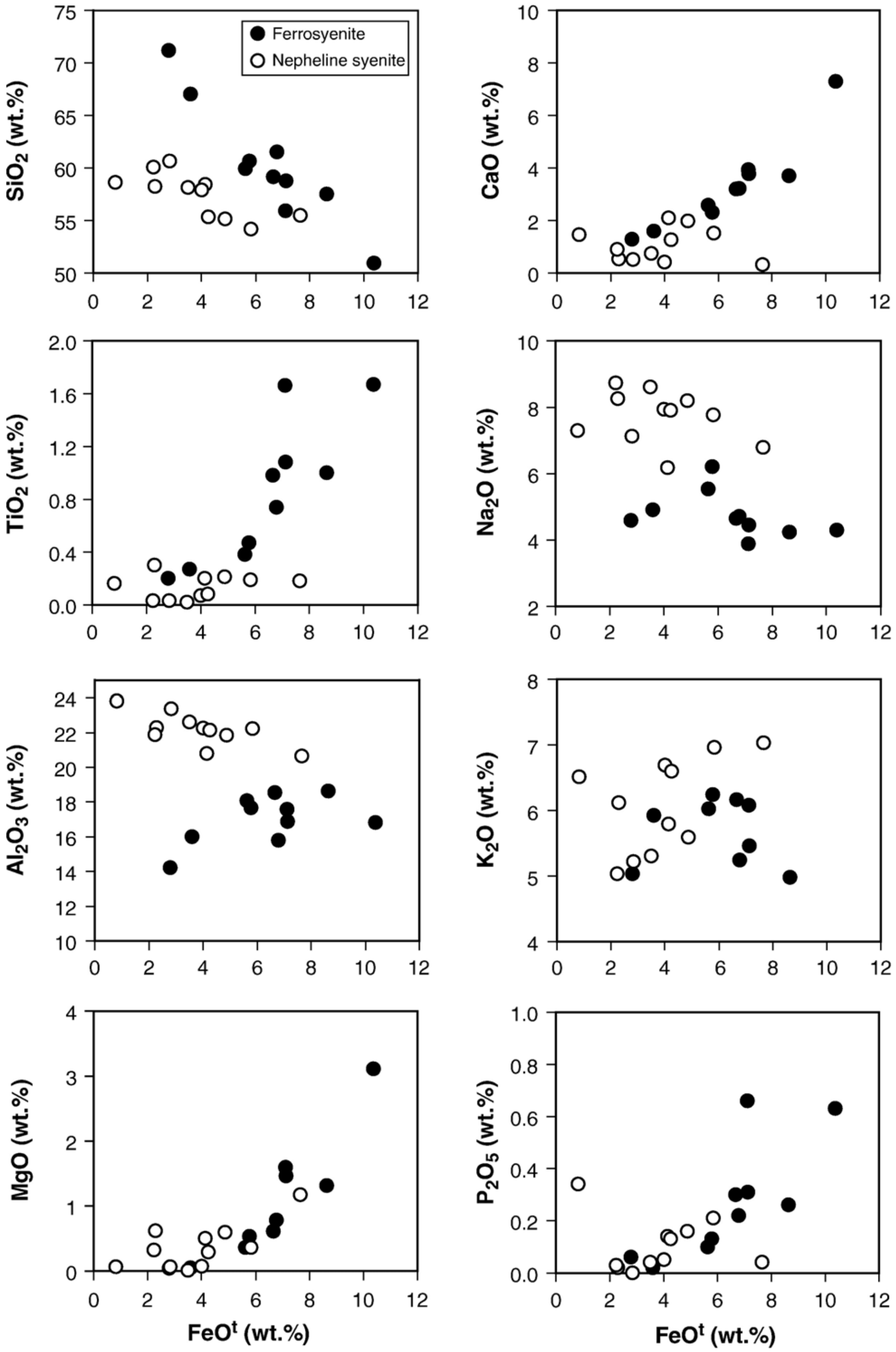

Fig. 11. Major element (wt.%) variation in the Errakonda ferrosyenite and Uppalapadu nepheline syenite with FeO^t as the monitor of differentiation.

shows a gradual decrease with FeO^t in the Errakonda but they do not show any characteristic trend in the Uppalapadu rocks. Sr and Ba show similar trends in both the rock types but with different slopes.

8.3. Rare earth elements

The chondrite-normalized REE pattern for the Chimakurti olivine clinopyroxenite (RBP 10) shows a mildly LREE-enriched pattern with a small but significant positive Eu anomaly (Table 6; Fig. 12A). Anorthosite (RBP 8), leuco-olivine gabbronorite (RBP 9) and gabbronorite (RBP 15) show low REE abundances, high Ce/Yb_N ratios and positive Eu anomalies (Table 6) characteristic of plagioclase-rich rocks. The presence of a positive Eu anomaly in the high-Al gabbroic dyke (RBP 6) provides evidence that the parental liquid to the Chimakurti cumulate rocks had a positive Eu anomaly.

Ferrodiorite from Errakonda (AMP1) exhibits a small positive Eu anomaly, a characteristic that is not uncommon in ferrosyenites associated with massif anorthosites (Mitchell et al., 1996a). Ferrosyenites (FSA2, RBP 30, RBP 28) display highly fractionated LREE and flat HREE patterns with negative Eu anomalies (Fig. 12B), compatible with extensive removal of plagioclase either during differentiation or during melting. With increasing amount of differentiation (as monitored by FeO^t) the abundances of the light REEs increase in the ferrosyenites and the negative Eu anomaly becomes increasingly more pronounced. Nepheline syenites of Uppalapadu have distinctly lower REE abundances than the ferrosyenites of Errakonda for similar FeO^t contents and lack negative Eu anomalies (Fig. 12C; Table 6).

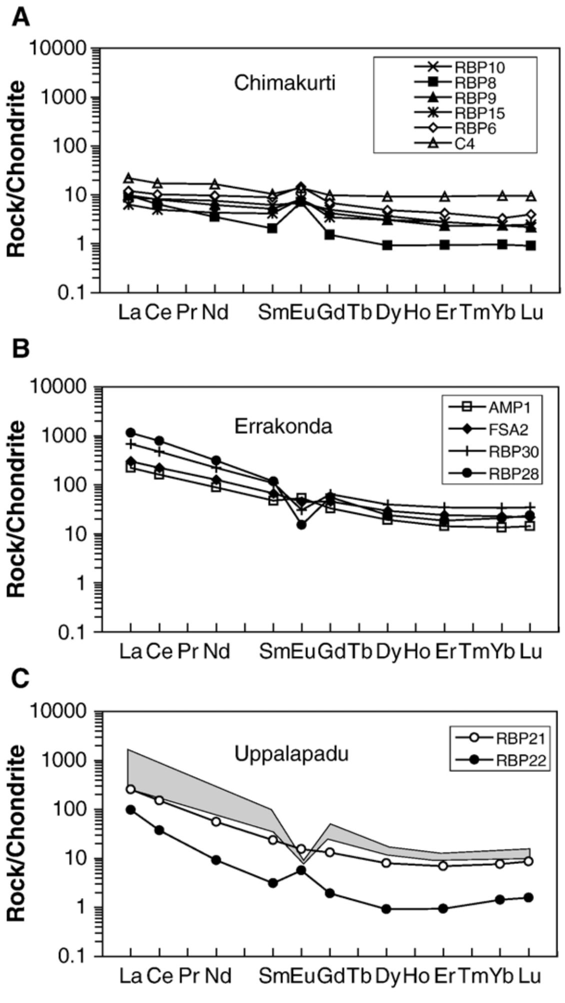

Fig. 12. Chondrite-normalized REE plots for Chimakurti (A), Errakonda (B) and Uppalapadu (C) rocks. Note that the REE abundances decrease with differentiation in the nepheline syenites. Normalizing values from Hanson (1980).

8.4. Rb–Sr and Sm–Nd isotopic systematics

Rb–Sr and Sm–Nd isotopic analyses were performed on rocks of the Chimakurti–Errakonda–Uppalapadu plutons and two potential contaminants to constrain their sources and effects of crustal contamination (Table 7). The mafic units of the Chimakurti pluton have high Sr (160–800 ppm) and low Nd (1.8–4.57 ppm) abundances whereas the ferrosyenite and nepheline syenite have low Sr (27–169 ppm) and high Nd (4–150 ppm). One consequence of this variation is that crustal assimilation will readily affect ε_{Nd} in the mafic rocks, whereas it will more strongly affect the Sr isotopic ratio of the ferrosyenite and nepheline syenite.

The I_{Sr} (calculated to 1352 Ma) for the clinopyroxenite, anorthosite, and gabbro of the Chimakurti pluton ranges from 0.70372 to 0.70494, with clinopyroxenite having the lowest and the marginal gabbronorite (RBP 15) having the highest I_{Sr} (Table 7; Fig. 13). I_{Sr} for ferrosyenite is considerably higher (I_{Sr}=.72174 to .77338). I_{Sr} in the nepheline syenite ranges from 0.71223 to 0.74814.

Age-corrected Nd isotopic ratios expressed in terms of ε_{Nd} range from 0.1 to −6.3 (Table 7). Within the Chimakurti pluton, the highest ε_{Nd} value is found in the clinopyroxenite and the lowest in the marginal gabbronorite (Table 7; Fig. 13). The nepheline syenite has ε_{Nd} ranging between −3.5 and −4.2; ε_{Nd} is only slightly more negative in the ferrosyenite, which has ε_{Nd}=−4.3 (Fig. 13). The distribution of ε_{Nd} and I_{Sr} values in the clinopyroxenite, anorthosite, and gabbro from the Chimakurti pluton can be explained by assimilation of small amounts (<10%) of rocks with isotopic compositions similar to that of the surrounding pelitic gneiss (Fig. 13). The same cannot be said for the ferrosyenite and nepheline syenite, both of which show a wide range of I_{Sr} at nearly constant ε_{Nd}.

9. Petrogenesis of the Chimakurti, Errakonda, and Uppalapadu plutons

9.1. Petrogenetic relationship of the A-type ferrosyenites to the nepheline syenite and gabbro–anorthosite suite

We have shown that the Errakonda ferrosyenite is coeval with the Uppalapadu nepheline syenite based on U–Pb zircon geochronology. Although there are no radiometric dates on the rocks in the Chimakurti pluton, we suggest that the 1352 Ma age for the Errakonda ferrosyenite is also the age for the Chimakurti pluton for the following reasons. Ferrosyenites (or mangarites) are commonly associated with anorthositic plutons and are interpreted to have formed from residual magmas of anorthositic plutons with various admixtures of crustal components (Kolker et al., 1991; Emslie et al., 1994; Scoates et al., 1996; Duchesne and Wilmart, 1997; Anderson et al., 2003). In such model, the Errakonda ferrosyenites would represent late stage differentiates of the magma that formed the clinopyroxenites, anorthosites, and gabbros of the Chimakurti pluton. Alternatively the ferrosyenites, like other A-type granitoids, could have formed by extreme differentiation of tholeiitic melts that were underplated beneath the crust at the same time as the parent magmas of the Chimakurti pluton were emplaced (Frost and Frost, 1997). The extreme iron enrichment of ferrosyenites, their extremely high temperature (in excess of 900 °C) and their low oxygen fugacity (FMQ or below) preclude a lower crustal source (Frost and Frost, 1997). We conclude that the ferrosyenites and gabbro–anorthosites are coeval and likely cogenetic.

The ferrosyenites cannot be petrologically related to the Ne–syenites. It is theoretically possible to derive both the Si-oversaturated and Si-undersaturated syenites from a common critically Si-undersaturated parental magma (Foland et al., 1993; Landoll et al., 1994). However, the ferrosyenite fractionated under relatively anhydrous, low f_{O_2} and high temperature conditions whereas the nepheline syenite crystallized under hydrous and high f_{O_2} and relatively lower temperature conditions. Additionally, our geochemical data clearly distinguishes the Errakonda ferrosyenite and Uppalapadu nepheline syenite. If these suites had a common parent, then the geochemical trends on variation diagrams would diverge from a common composition with a high FeO^t. Excepting Al_2O_3, none of the other oxides show such a divergence (Fig. 11). In addition, the REE patterns and abundances at any given FeO^t are distinct for the two series (Fig. 12; Tables 5 and 6).

Table 7
Sr and Nd isotopic data for Chimakurti–Errakonda–Uppalapadu plutons and country rocks

Sample	Pluton	Rock name	Rb (ppm)	Sr (ppm)	$^{87}Rb/^{86}Sr$	$^{87}Sr/^{86}Sr$	$I_{Sr}^{1352\ Ma}$	Sm (ppm)	Nd (ppm)	$^{147}Sm/^{144}Nd$	$^{143}Nd/^{144}Nd$	$Nd_i^{1352\ Ma}$	$\varepsilon_{Nd}^{1352\ Ma}$
RBP 10	C	Olivine clinopyroxenite	2.25	160.30	0.0406	0.70451	0.70372	0.87	3.47	0.15164	0.5122423	0.510895	0.1
RBP 8	C	Anorthosite	1.62	801.61	0.0059	0.70402	0.70391	0.33	1.84	0.10836	0.5116256	0.510663	−4.5
RBP 9	C	Leuco-olivine gabbronorite	1.21	518.80	0.0068	0.70408	0.70395	0.76	3.15	0.14658	0.5119912	0.510689	−3.9
RBP 4	C	Olivine gabbronorite	1.56	573.47	0.0079	0.70419	0.70404	0.41	1.85	0.13577	0.5119024	0.510697	−3.8
RBP 15	C	Gabbronorite	1.30	726.42	0.0052	0.70504	0.70494	0.62	2.22	0.16992	0.5120769	0.510568	−6.3
RBP 6	C	High-Al gabbro dyke	0.98	575.69	0.0049	0.70397	0.70388	1.19	4.57	0.15723	0.5122224	0.510826	−1.3
RBP 28	E	Ferrosyenite	87.49	26.61	9.7514	0.96240	0.77338	17.20	150.29	0.06919	0.5112846	0.510670	−4.3
RBP 30	E	Ferrosyenite	77.08	159.51	1.4039	0.74895	0.72174	16.52	111.52	0.08960	0.5114663	0.510670	−4.3
RBP 21	U	Nepheline syenite	108.53	28.65	11.2387	0.96599	0.74814	0.43	4.44	0.05821	0.5112267	0.510710	−3.5
RBP 22	U	Nepheline syenite	99.34	169.29	1.7044	0.74527	0.71223	3.43	27.37	0.07586	0.5113493	0.510676	−4.2
RBP 3	Country rock	Archean metapelite	20.90	162.77	0.3732	0.75177	0.74454	9.49	53.05	0.10810	0.5112790	0.510319	−11.2
RBP 24	Country rock	Archean gneiss						5.28	11.5	0.27787	0.5130540	0.510586	−6.0

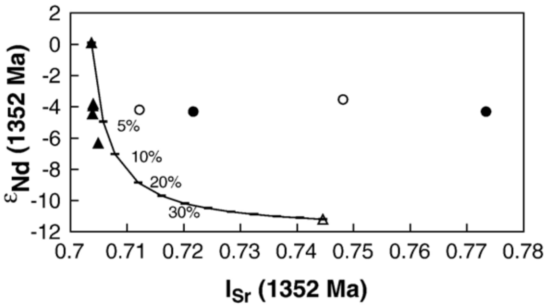

Fig. 13. Initial ε_{Nd} vs. I_{Sr} diagrams for representative rocks of the Chimakurti–Errakonda–Uppalapadu plutons. Cumulate rocks (filled triangles; clinopyroxenites, anorthosites and gabbros) show wide variation in ε_{Nd} for a limited range in I_{Sr}. Binary mixing calculations suggest less than 10% contamination of the primitive sample of the CAG suite by Archean metapelite or its anatectic melts (open triangle). Note the extremely high I_{Sr} in some of the syenites (open circles = nepheline syenite, filled circles = ferrosyenite).

Therefore, on these petrological grounds, we suggest that the Errakonda ferrosyenite has no genetic relationship with the Uppalapadu nepheline syenite.

9.2. Parental liquids to the Chimakurti and Uppalapadu plutons

9.2.1. Chimakurti (tholeiitic suite)

We have calculated the equilibrium liquid trace and minor element compositions for the Chimakurti pluton using published mineral/melt partition coefficients and the equation $C_L = C_S/D$. Details of the calculation procedure are given in the caption to Fig. 14. The calculated trace element compositions are shown as MORB-normalized spidergrams (Fig. 14). Our cumulate inversions appear to be successful because clinopyroxenite (with > 75% modal clinopyroxene) and anorthosite (with > 85% modal plagioclase) cumulates have yielded identical liquid trace element patterns (Fig. 14). Other cumulates also yielded similar liquid analogues but with higher absolute abundances. We have also plotted the incompatible elemental composition of the high-Al gabbroic dyke (RBP 6; Tables 5 and 6) and both observed and calculated parental liquid trace element compositions to the massif-type anorthosites (Markl and Frost, 1999; Bedard, 2001). The similarity in trace elements among the high-Al gabbroic dyke, the calculated equilibrium liquid compositions to the cumulate rocks of the Chimakurti pluton and the parental liquids to the massif-type anorthosite plutons strongly support the affinity of the Chimakurti pluton to the massif anorthosites. Troughs for Nb, P and Ti in the parental liquids may be the result of plagioclase-rich nature of the parental liquid, possibly further accentuated by crustal contamination. Major element composition of the high-Al gabbroic dyke is similar to high-Al tholeiitic magmas that are presumed as parental magmas of other Proterozoic massif anorthosite complexes (Berg, 1980; Emslie, 1980; Morse, 1981; Olson, 1992; Mitchell et al., 1995; Markl and Frost, 1999; Scoates and Mitchell, 2000).

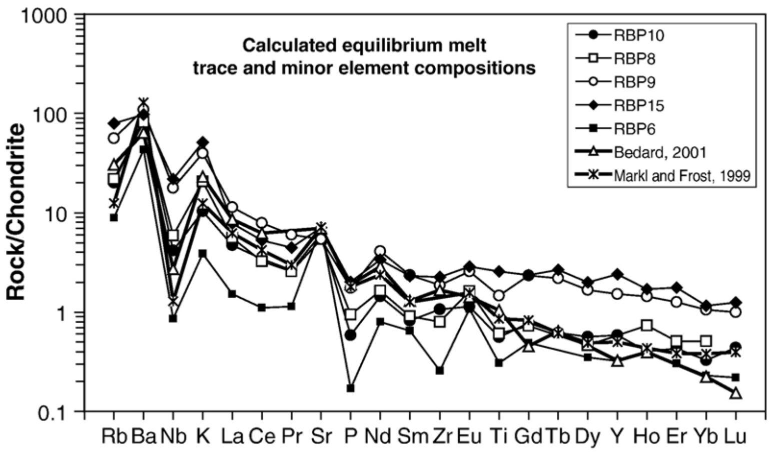

Fig. 14. MORB-normalized equilibrium liquid trace and minor element compositions for the Chimakurti cumulates. The liquids are given same numbers as corresponding cumulates. MORB normalizing values are after Sun and McDonough (1989). Liquid trace element compositions are calculated by using the equation $C_L = C_S/D$ and published mineral/melt partition coefficients (Bedard, 2001; Claeson and Meurer, 2004). C_L is the concentration of element in the equilibrium liquid, C_S is the concentration of element in the solid (cumulate rock) and D is the bulk distribution coefficient ($\sum X_i Kd_i$); X_i is the modal abundance of phase i in the solid and Kd_i is mineral/melt partition coefficient of element in phase i. Percentage of estimated intercumulus liquid is substituted as a phase in X_i with Kd_i equals to 1. Both observed and calculated parental liquid trace element compositions to the massif-type anorthosites (Markl and Frost, 1999; Bedard, 2001) are also shown for comparison. For discussion, see the text.

9.2.2. Uppalapadu (alkaline suite)

In the absence of any mesocratic/melanocratic cogenetic members, it is difficult to specify the parent magma from which the nepheline syenites were produced. Nepheline syenites may be derived by fractional crystallization of alkali basaltic, nephelinitic/basanitic or potassic alkaline parental magmas (Sørenson, 1974; Fitton and Upton, 1987; Leat et al., 1988; Mitchell, 1996; Mitchell et al., 1996b) or by small degree melting of mantle and/or crustal rocks (Bailey, 1974; Price et al., 1985). Nepheline syenites derived from alkali basalts characteristically show negative Eu anomalies that increase with increasing REE abundances, indicating control by plagioclase fractionation (Fig. 15A). In contrast, nepheline syenites derived from nephelinitic/basanitic and potassic alkaline magmas show little or no Eu anomaly (Fig. 15B, C). Because the nepheline syenites of Uppalapadu and those of other nepheline syenite bodies of the Prakasam Alkaline Province lack negative Eu anomaly (Fig. 15D), we conclude that the nepheline syenites of the Uppalapadu were not derived from alkali basaltic magmas.

The nepheline syenites of Uppalapadu are sodic ($Na_2O/K_2O>1$) and show typical *miascitic* character (molar $Na_2O+K_2O/Al_2O_3<1$ and absence of alkalic amphibole and pyroxene). The presence of modal corundum and hercynite in the nepheline syenite demonstrates its metaluminous to peraluminous nature. Miascitic nepheline syenites are considered to be derived by fractional crystallization of alkali basaltic or basanitic parental melts (Baker, 1987; Jung, 1995; Morogan et al., 2000). Since we have already demonstrated that alkali basalt cannot be a parental melt to the nepheline syenites of Uppalapadu, we infer that they have been derived from basanitic parental liquids. High-pressure fractionation of Ti-rich amphibole and clinopyroxene along with minor amounts of olivine and phlogopite from basanitic liquids produce phonolitic magmas that crystallize to form mesocratic nepheline syenites (Irving and Green, 1972; Green et al.,

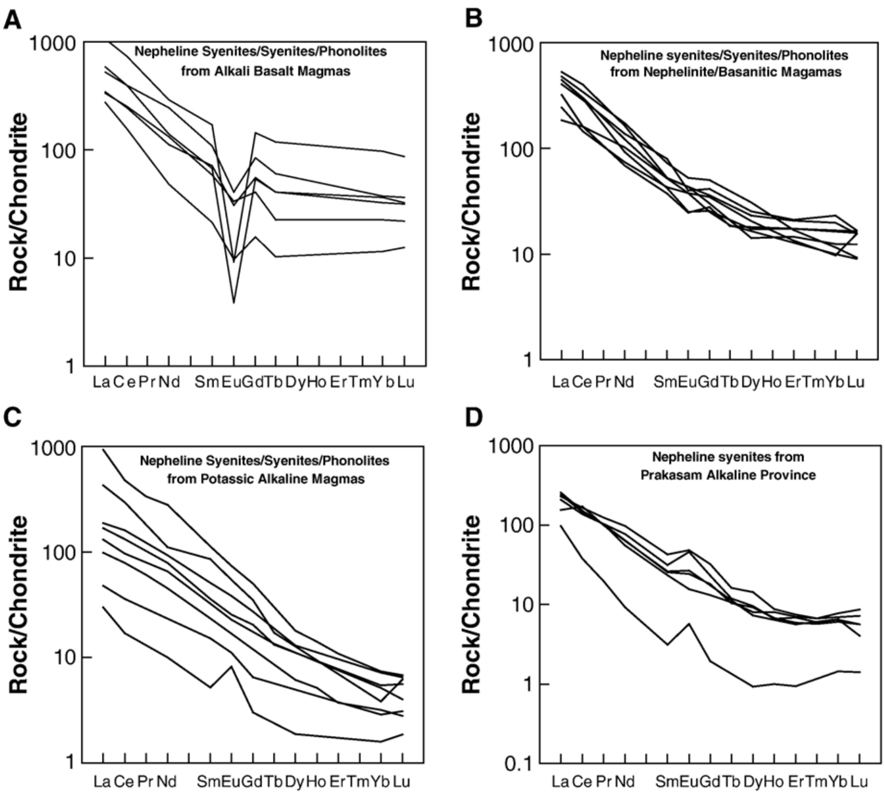

Fig. 15. Chondrite-normalized REE patterns for nepheline syenites (and phonolites) derived from alkali basalt (A), nephelinite/basanite (B) and potassic alkaline (C) parental liquids. Nepheline syenites of Prakasam Alkaline Province (including present study, bold lines) are shown in (D). All data normalized to values from Hanson (1980). Sources of data for (A): Kyle et al. (1992), Weis et al. (1993) and Panter et al. (1997); for (B): Wittke and Mack (1993), Jung (1995) and Potter (1996); for (C): Leat et al. (1988), Thomson and Fowler (1986), Thomson et al. (1990), Bourne and L'Heureux (1991) and O'Brien et al. (1995); for (D): Ratnakar and Vijaya Kumar (1995), present study and unpublished data of authors (3 analyses from Purimetla).

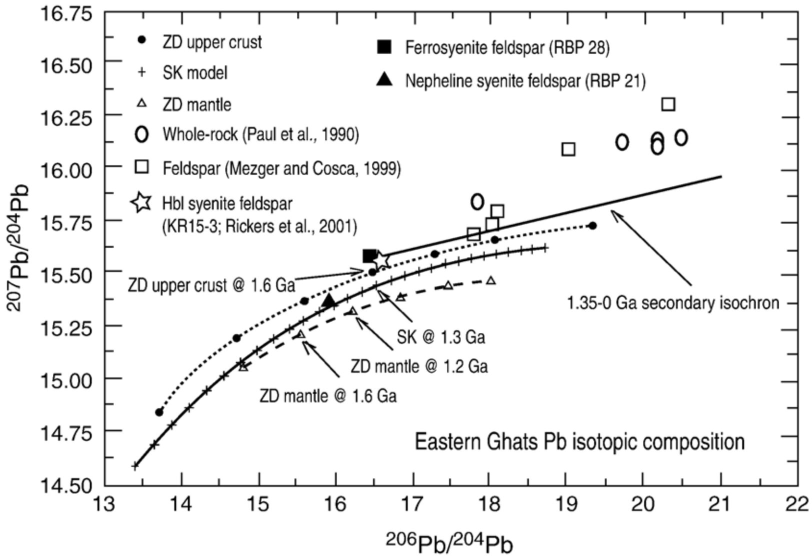

Fig. 16. Pb isotopic composition in the feldspars from ferrosyenite (RBP 28) and nepheline syenite (RBP 21) from the Errakonda–Uppalapadu plutons. For comparison Pb isotopic data of feldspars (Mezger and Cosca, 1999) and whole-rocks (Paul et al., 1990) from EGB granulites, and feldspar from a hornblende syenite (KR15-3; Rickers et al., 2001) from the present study area are also plotted. Also plotted are model evolution curves: SK = Stacey and Kramers (1975), ZD = Zartman and Doe (1981).

1974). Such a plagioclase-absent fractionation model has been proposed for the origin of Kasunga–Chipala nepheline syenite of Malawi alkaline province (Eby et al., 1998) and Ditrau (Ditro) alkaline complex of Romania (Morogan et al., 2000). Fractionation dominated by the mafic phases results in the lack of a negative Eu anomaly and high Al_2O_3 contents in the evolved syenitic melts. Additionally, saturation of the parental basanitic melt in accessory phases such as allanite, titanate or apatite results in decrease of commonly considered incompatible elements (for e.g. REE) with differentiation (Upadhyay et al., 2006, and references cited therein). Thus, it is most likely that the parental melt for Uppalapadu nepheline syenite is basanitic in composition. Similar conclusions are drawn for the Elchuru nepheline syenite located north of the Uppalapadu pluton (Upadhyay et al., 2006).

9.3. Crustal contamination of Chimakurti, Errakonda, and Uppalapadu plutons

The possible crustal contaminants for the Chimakurti, Errakonda, and Uppalapadu plutons at the present level of emplacement are metapelite and granite gneiss, which are in direct contact with the plutons and have lower dry solidii than the other country rocks such as amphibolite, quartzite and biotite–garnet schist. Moreover, evidence of partial melting of metapelite is

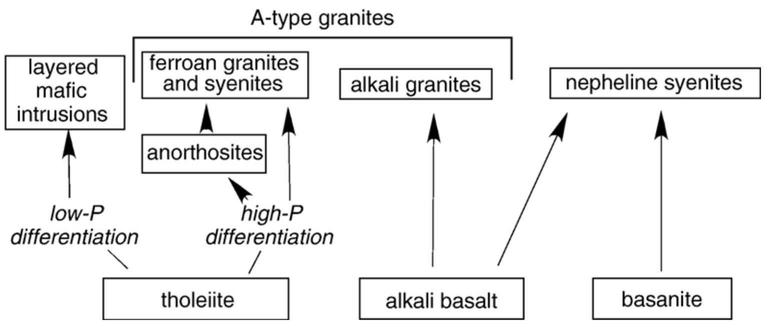

Fig. 17. Model for the generation of intraplate magmatic suites. Although ferroan granites and alkali granites are commonly associated and together comprise the A-type granites, the temporal and spatial association of plutonic complexes derived from tholeiitic and basanitic magmatism, such as found in the Chimakurti, Errakonda, and Uppalapadu plutons, is rare.

recorded in the contact aureole around the Chimakurti pluton (Babu, 1996; Dasgupta et al., 1997). Based on the phlogopite coronas present in the Ravipadu gabbros located south of Chimakurti (Fig. 2), Vijaya Kumar and Ratnakar (1999) have suggested that K_2O and Al_2O_3 are the dominant cations added to the basic magma from the metapelites. These gabbros also have higher abundances of incompatible elements than the simple fractional crystallization models predict (Vijaya Kumar and Ratnakar, 2001). Addition of K_2O and Al_2O_3 to the basic magma may form modal biotite, which could deplete the remaining melt in olivine component and thus lead to an increase in modal hypersthene. Indeed these features also are observed in the Chimakurti pluton: within a meter from the margin the gabbronorite grade into norite with a concomitant increase in modal plagioclase and occurrence of biotite.

Nd and Sr isotope compositions indicate that three plutons assimilated crustal components as they differentiated. The ε_{Nd} variation among the clinopyroxenite, anorthosite, and gabbro of the Chimakurti pluton (0.09 to −6.2) may have been caused by between 0 and 10% bulk assimilation of a contaminant with isotopic compositions similar to Archean metapelite (Fig. 13). Ferrosyenites have ε_{Nd} values similar to some of the gabbroic rocks, but much higher Nd concentrations. For this reason, the effects of assimilation of country rocks are less apparent in the ε_{Nd} values of ferrosyenites. The role of crustal assimilation in producing the negative ε_{Nd} values for the nepheline syenites must be limited, since it could drive the liquid composition towards Si-saturation. It seems likely that the negative ε_{Nd} values for the nepheline syenites are their original traits reflecting those of the parental liquids and their sources.

Further evidence for the crustal contamination of the Errakonda and Uppalapadu rocks comes from the Pb isotopic data from feldspars of ferrosyenite (RBP 28) and nepheline syenite (RBP 21). Feldspars from the ferrosyenite have higher $^{206}Pb/^{204}Pb$ and $^{207}Pb/^{204}Pb$ ratios than those of the nepheline syenite (Fig. 16). Though the feldspars from these rocks are much less radiogenic than those from the granulite facies rocks of the Eastern Ghats Belt (Paul et al., 1990; Mezger and Cosca, 1999; Rickers et al., 2001), they still plot above the mantle Pb isotopic composition at 1.35 Ga (Zartman and Doe, 1981; Fig. 16), suggesting interaction with an older crustal reservoir. The Pb isotopic data further suggest that this older crustal reservoir had a high μ ($^{238}U/^{204}Pb$). A hornblende syenite (KR15-3) collected from the present study area (Rickers et al., 2001) has a similar Pb isotopic composition to that of metapelites. Rickers et al. (2001) have interpreted this feature in terms of contamination of juvenile mantle melts with old crust. However, the extremely radiogenic initial $^{87}Sr/^{86}Sr$ of ferrosyenite sample RBP 28 exceeds that of any analyzed metapelite sample from the Ongole domain (Rickers et al., 2001). One possible process that might produce such an extreme composition is the interaction of the ferrosyenite melt with Sr-rich melts derived due to dehydration melting of the biotite during contact metamorphism of metapelite. A similar mechanism has been suggested to explain the extreme Sr isotopic compositions of marginal mafic granulites bordering the Nain plutonic suite (Royse et al., 1999).

10. Conclusions

Magmatism in continental rifts leads to a wide variety of basaltic magmas, from tholeiitic to highly alkalic. The way that these magmas may be related to plutonic rock suites found in intraplate environments is shown schematically in Fig. 17. Tholeiitic magmas emplaced at shallow levels may differentiate to layered mafic intrusions such as the Skaergaard or Bushveld intrusions. The same magmas emplaced at depth will result in massif anorthosites and their differentiates (Emslie, 1985; Longhi and Ashwal, 1985). High pressure differentiation of tholeiitic rocks will also result in potassic, ferroan granites (Frost et al., 2001b; Nekvasil et al., 2001). Alkali basalts may differentiate to nepheline syenites, if there is sufficient crustal assimilation, to alkali granites. More alkalic basalts, such as basanites will also evolve to nepheline syenites, although, as we noted above, these nepheline-rich rocks will be geochemically distinct from those produced by alkali basalts.

Ferroan alkalic or alkali–calcic granites are not uncommonly associated with alkali granites (Smith et al., 1999a,b) and these two granite types are commonly called A-type granites. Although nepheline syenites, like A-type granites and anorthosites, may form in a rifting environment, the two associations are seldom found together. The 1352 Ma magmatism in the Eastern Ghats is unusual in that it documents a spatial and temporal association of these extreme endmembers of continental rift magmatism.

Acknowledgements

KVK is thankful to Dr. J. Ratnakar for his help during the fieldwork and Dr. E.V.S.S.K. Babu for general help. We acknowledge Dr. Susan M. Swapp for assistance with the electron microprobe analyses. KVK gratefully acknowledges the Department of Science and Technology (Science and Engineering Research Council), Government of India, for awarding the BOYSCAST Fellowship. He wishes to thank his parent institute (SRTM University, Nanded) for granting the sabbatical leave and the staff at the Department of Geology and Geophysics, University of Wyoming for their support and assistance. CDF and BRF acknowledge NSF grants EAR9706237 and EAR9909260.

References

Aftalion, M., Bowes, D.R., Dash, B., Dempster, T.J., 1988. Late Proterozoic charnockites in Orissa, India: a U–Pb and Rb–Sr isotopic study. Journal of Geology 96, 663–676.

Aftalion, M., Bowes, D.R., Dash, B., Fallick, A.E., 2000. Late Pan-African thermal history in the Eastern Ghats Terrane, India, from U–Pb and K–Ar isotopic study of the Mid-Proterozoic Khariar alkali syenite, Orissa. Geological Survey of India Special Publication 57, 26–33.

Andersen, D.J., Lindsley, D.H., Davidson, P.M., 1993. QUILF: a Pascal program to assess equilibria among Fe–Mg–Ti oxides, pyroxene, olivine, and quartz. Computers and Geosciences 19, 1333–1350.

Anderson, I.C., Frost, C.D., Frost, B.R., 2003. Petrogenesis of the Red Mountain pluton, Laramie anorthosite complex, Wyoming: implications for the origin of A-type granite. Precambrian Research 124, 243–267.

Arndt, N.T., Chauvel, C., Czamanske, G., Fedorenko, V., 1998. Two mantle sources, two plumbing systems: tholeiitic and alkaline magmatism of the Maymecha river basin, Siberian flood volcanic province. Contributions to Mineralogy and Petrology 133, 297–313.

Babu, E.V.S.S.K., 1996. Petrological studies on the Chimakurti gabbro–anorthosite–olivine–clinopyroxenite complex and its contact aureole, India. PhD Thesis, University of Cambridge.

Babu, E.V.S.S.K., Leelanandam, C., 1993. Fossil pigeonites and exsolution features in pyroxenes from ferrosyenites of South India. Journal of the Geological Society of India 41, 351–359.

Babu, E.V.S.S.K., Vijaya Kumar, K., Pyle, D.M., 1997. Spinel (hercynite) adcumulate from the Chimakurti gabbro–anorthosite pluton, Prakasam District, Andhra Pradesh, India: evidence for plagioclase buoyancy and magma mixing. Current Science 73, 441–444.

Bailey, D.K., 1974. Continental rifting and alkaline magmatism. In: Sørenson, H. (Ed.), The Alkaline Rocks. Wiley, New York, pp. 148–159.

Baker, B.H., 1987. Outline of the petrology of the Kenya Rift alkaline province. In: Fitton, J.G., Upton, B.G.J. (Eds.), Alkaline Igneous Rocks. Geological Society Special Publication, vol. 30, pp. 1–13.

Bedard, J.H., 2001. Parental magmas of the Nain plutonic suite anorthosites and mafic cumulates: a trace element modeling approach. Contributions to Mineralogy and Petrology 141, 747–771.

Berg, J.H., 1980. Snowflake troctolite in the Hettasch intrusion, Labrador: evidence for magma-mixing and supercooling in a plutonic environment. Contributions to Mineralogy and Petrology 72, 339–351.

Bhattacharyya, S., Bose, S.K., Dutta, H.S., 1981. Petrology of the alkalic suite of Errakonda hill near Chimakurti, Prakasam District, Andhra Pradesh. Indian Journal of Earth Sciences 9, 84–89.

Bourne, J.H., L'Heureux, M., 1991. The petrography and geochemistry of the Clericy pluton: an ultrapotassic pyroxenite–syenite suite of late Achaean age from the Abitibi region, Quebec. Precambrian Research 52, 37–51.

Chamberlain, K.R., Bowring, S.A., 2001. Apatite–feldspar U–Pb thermochronometer: a reliable, mid-range (∼450 °C), diffusion-controlled system. Chemical Geology 172, 173–200.

Claeson, D.T., Meurer, W.P., 2004. Fractional crystallization of hydrous basaltic "arc-type" magmas and the formation of amphibole-bearing gabbroic cumulates. Contributions to Mineralogy and Petrology 147, 288–304.

Czygan, W., Goldenberg, G., 1989. Petrography and geochemistry of the alkaline complexes of Sivamalai, Elchuru and Uppalapadu, India. In: Leelanandam, C. (Ed.), Alkaline Rocks. Memoir Geological Society of India, vol. 15, pp. 225–240.

Dasgupta, S., Ehl, J., Raith, M.M., Sengupta, P., Sengupta, P., 1997. Midcrustal contact metamorphism around the Chimakurthy mafic–ultramafic complex, Eastern Ghats Belt, India. Contributions to Mineralogy and Petrology 129, 182–197.

De Albuquerque, C.A.R., 1973. Geochemistry of biotites from granitic rocks, northern Portugal. Geochimica et Cosmochimica Acta 37, 1779–1802.

Dobmeier, C.J., Lütke, S., Hammerschmidt, K., Mezger, K., 2006. Emplacement and deformation of the Vinukonda meta-granite (Eastern Ghats, India)—implications for the geological evolution of peninsular India and for Rodinia reconstructions. Precambrian Research 146, 165–178.

Dobmeier, C.J., Raith, M.M., 2003. Crustal architecture evolution of the Eastern Ghats Belt and adjacent regions of India. In: Yoshida, M., Windley, B.F., Dasgupta, S. (Eds.), Proterozoic East Gondwana: Supercontinent Assembly and Breakup. Geological Society Special Publication, vol. 206, pp. 145–168.

Duchesne, J.-C., Wilmart, E., 1997. Igneous charnockites and related rocks from the Bjerkreim–Sokndal layered intrusion (southwest Norway): a jotunite (hypersthene monzodiorite)-derived A-type granitoid suite. Journal of Petrology 38, 337–369.

Duke, N.A., Edgar, A.D., 1977. Petrology of the Blue Mountain and Bigwood felsic alkaline complexes of the Grenville province of Ontario. Canadian Journal of Earth Sciences 14, 515–538.

Eby, G.N., Woolley, A.R., Din, V., Platt, R.G., 1998. Geochemistry and petrogenesis of nepheline syenites: Kasunga–Chipala, Ilomba and Ulindi nepheline syenite intrusions, North Nyasa Alkaline province, Malawi. Journal of Petrology 39, 1405–1424.

Elkins, L.T., Grove, T.L., 1990. Ternary feldspar experiments and thermodynamic models. American Mineralogist 75, 544–559.

Elthon, D., Scarfe, C.M., 1984. High-pressure phase equilibria of a high-magnesia basalt and the genesis of primary oceanic basalts. American Mineralogist 69, 1–15.

Emslie, R.F., 1980. Geology and petrology of the Harp Lake Complex, Central Labrador: an example of Elsonian magmatism. Geol. Surv. of Canada Bull., vol. 293. 136 pp.

Emslie, R.F., 1985. Proterozoic anorthosite massifs. In: Tobi, AC., Touret, J.L.R. (Eds.), The Deep Proterozoic Crust in the North American Provinces. D. Reidel Publishing Co., pp. 39–60.

Emslie, R.F., Hamilton, M.A., Theriault, R.J., 1994. Petrogenesis of a Mid-Proterozoic anorthosite–mangerite–charnockite–granite (AMCG) complex: Isotopic and chemical evidence from the Nain plutonic suite. Journal of Geology 102, 539–558.

Finch, A.A., Parsons, I., Mingard, S.C., 1995. Biotites as indicators of fluorine fugacities in late-stage magmatic fluids: the Gardar Province of South Greenland. Journal of Petrology 36, 1701–1728.

Fitton, J.G., Upton, B.G.J. (Eds.), 1987. Alkaline Igneous Rocks. Geol. Soc. Lond. Special Publication, vol. 30. Blackwell, Oxford.
Foland, K.A., Landoll, J.D., Henderson, C.M.B., Jiangfeng, C., 1993. Formation of cogenetic quartz and nepheline syenites. Geochimica et Cosmochimica Acta 57, 697–704.
Frost, B.R., Barnes, C.G., Collins, W.J., Arculus, R.J., Ellis, D.J., Frost, C.D., 2001a. A geochemical classification for granitic rocks. Journal of Petrology 42, 2033–2048.
Frost, C.D., Bell, J.M., Frost, B.R., Chamberlain, K.R., 2001b. Crustal growth by magmatic underplating: isotopic evidence from the northern Sherman batholith. Geology 29, 515–518.
Frost, B.R., Lindsley, D.H., 1992. Equilibria among Fe–Ti oxides, pyroxenes, olivine, and quartz: Part II. Application. American Mineralogist 77, 1004–1020.
Frost, C.D., Frost, B.R., 1997. Reduced rapakivi-type granites: the tholeiitic connection. Geology 25, 647–650.
Frost, B.R., Frost, C.D., Hulsebosch, T.P., Swapp, S.M., 2000. Origin of the charnockites of the Louis Lake Batholith, Wind River Range, Wyoming. Journal of Petrology 41, 1759–1776.
Giret, A., Lameyre, J., 1985. Inverted alkaline–tholeiitic sequences related to lithospheric thickness in the evolution of continental rifts and ocean islands. Journal of African Earth Sciences 3, 261–268.
Green, D.H, Ringwood, A.E., 1967. The genesis of basaltic magmas. Contributions to Mineralogy and Petrology 15, 103–190.
Green, D.H., Edgar, A.D., Beasley, P., Kiss, E., Ware, N.G., 1974. Upper mantle source for some hawaiites, mugearites and benmorites. Contributions to Mineralogy and Petrology 48, 33–43.
Grew, E.S., Manton, W.J., 1986. A new correlation of sapphirine granulites in the Indo-Antarctic metamorphic terrain: Late Proterozoic dates from the Eastern Ghats Province of India. Precambrian Research 33, 123–137.
Guidotti, C.V., Cheney, J.T., Conatore, P.D., 1975. Interrelationship between Mg/Fe ratio and octahedral Al content in biotite. American Mineralogist 60, 849–853.
Gupta, J.N., Pandey, B.K., Chabria, T., Banerjee, D.C., Jayaram, K.M.V., 1984. Rb–Sr geochronological studies on the granites of Vinukonda and Kanigiri, Prakasam District, Andhra Pradesh, India. Precambrian Research 26, 105–109.
Hamilton, D.L., 1961. Nephelines as crystallization temperature indicators. Journal of Geology 69, 321–329.
Hanson, G.N., 1980. Rare earth elements in petrogenetic studies of igneous systems. Annual Review Earth and Planetary Sciences 8, 371–406.
Harris, N.B.W., 1974. The petrology and petrogenesis of some muscovite granite sills from the Brousse massif, Central Pyrenees. Contributions to Mineralogy and Petrology 45, 215–230.
Henderson, C.M.B., Pendlebury, K., Foland, K.A., 1989. Mineralogy and petrology of the Red Hill alkaline igneous complex, New Hampshire, USA. Journal of Petrology 30, 627–666.
Irving, A.J., Green, D.H., 1972. Experimental study of phase relationships in a high-pressure mugearitic basalt as a function of water content, Abstracts with Programs. Geological Society of America 4, 550–551.
Joyce, A.S., 1973. Chemistry of the minerals of the granitic Murrumbidgee batholith, Australian Capital Territory. Chemical Geology 11, 271–296.
Jung, S., 1995. Geochemistry and petrogenesis of rift-related Tertiary alkaline rocks from the Rhon area (central Germany). Neues Jahrbuch fur Mineralogie Abhandlungen 169, 193–226.
Kolker, A., Frost, C.D., Hanson, G.N., Geist, D.J., 1991. Neodymium, strontium, and lead isotopes in the Maloin Ranch Pluton, Wyoming: implications for the origin of evolved rocks at anorthosite margins. Geochimica et Cosmochimica Acta 55, 2285–2297.
Kovach, V.P., Berezhnaya, N.G., Salinikova, E.B., Narayana, B.L., Divakara Rao, V., Yoshida, M., Korov, A.B., 1998. U–Pb zircon age and Nd isotope systematics of megacrystic charnockites in the Eastern Ghats Granulite Belt, India, and their implication for East Gondwana reconstruction. Journal of African Earth Sciences 27, 125–127.
Kovach, V.P., Simmat, R., Rickers, K., Berezhnaya, N.G., Salnikova, E.B., Dobmeier, C., Raith, M.M., Yakovleva, S.Z., Kotov, A.B., 2001. The Western Charnockite Zone of the Eastern Ghats Belt, India: an independent crustal province of late Archean (2.8 Ga) and Paleoproterozoic (1.7–1.6 Ga) terrains. Gondwana Research 4, 666–667.
Krause, O., Dobmeier, C., Raith, M.M., Mezger, K., 2001. Age of emplacement of massif-type anorthosites in the Eastern Ghats Belt, India: constraints from U–Pb zircon dating and structural studies. Precambrian Research 109, 25–38.
Krishna Reddy, K., Ratnakar, J., Leelanandam, C., 1998. A petrochemical study of the Proterozoic alkaline complex of Uppalapadu, Prakasam Province, Andhra Pradesh, India. Journal of the Geological Society of India 52, 41–52.
Krogh, T.E., 1973. A low-contamination method for hydrothermal decomposition of zircon and extraction of U and Pb for isotopic age determination. Geochimica et Cosmochimica Acta 37, 485–494.
Kyle, P.R., Moore, J.A., Thirlwall, M.F., 1992. Petrologic evolution of anorthoclase phonolite lavas at Mount Erebus, Ross Island, Antarctica. Journal of Petrology 33, 849–875.
Landoll, J.D., Foland, K.A., Henderson, C.M.B., 1994. Nd isotopes demonstrate the role of contamination in the formation of coexisting quartz and nepheline syenites at the Abu Khrug complex, Egypt. Contributions to Mineralogy and Petrology 117, 305–329.
Leat, P.T., Thomson, R.N., Morrison, M.A., Hendry, G.L., Dickin, A.P., 1988. Silicic magmas derived by fractional crystallization of Miocene minette, Elkhead Mountains, Colorado. Mineralogical Magazine 52, 577–585.
Leelanandam, C., 1989. The Prakasam Alkaline Province in Andhra Pradesh, India. Journal of the Geological Society of India 34, 25–45.
Leelanandam, C., 1993a. Eulitic and ferrosilitic orthopyroxenes from ferrosyenites of south India: evidences for a high temperature crystallization and tholeiitic parentage. Current Science 64, 729–735.
Leelanandam, C., 1993b. Almandine-rich garnets from fayalite–ferrosilite–quartz-bearing ferrosyenites in the Prakasam District of Andhra Pradesh, India. Journal of the Geological Society of India 41, 437–443.
Leelanandam, C., 1994. Na-poor ferro-augites and ferro-hedenbergites from ferrosilite-bearing ferrosyenites of the Prakasam District in Andhra Pradesh, India: further evidences for a tholeiitic parentage. Journal of the Geological Society of India 44, 7–16.
Longhi, J., Ashwal, L.D., 1985. Two-stage model for lunar and terrestrial anorthosites: petrogenesis without a magma ocean. Proc. 15 Lunar and Planetary Science Conference, Part 2. Journal of Geophysical Research 90, C571–C584.
Ludwig, K.R., 1988. PBDAT for MS-DOS, a computer program for IBM-PC compatibles for processing raw Pb–U–Th isotope data, revised June, 1993. US Geological Survey Open-File Rep. 88–542.
Ludwig, K.R., 1991. ISOPLOT for MS-DOS, a plotting and regression program for radiogenic isotope data, for IBM-PC compatible

computers, revised October, 1994. US Geological Survey Open-File Rep. 91–445.

Markl, G., Frost, B.R., 1999. The origin of anorthosites and related rocks from Lofoten Islands, northern Norway: II. Calculation of parental liquid compositions from anorthosites. Journal of Petrology 40, 61–77.

Mezger, K., Cosca, M.A., 1999. The thermal history of the Eastern Ghats Belt (India) as revealed by U–Pb and $^{40}Ar/^{39}Ar$ dating of metamorphic and magmatic minerals: implications for the SWEAT correlation. Precambrian Research 94, 251–271.

Mitchell, R.H., 1996. Undersaturated potassic plutonic complexes. In: Mitchell, R.H. (Ed.), Undersaturated Alkaline Rocks: Mineralogy, Petrogenesis, and Economic Potential. Mineralogical Association of Canada, Short Course Series, vol. 24, pp. 193–216.

Mitchell, J.N., Scoates, J.S., Frost, C.D., 1995. High-Al gabbros in the Laramie anorthosite complex, Wyoming: implications for the composition of melts parental to Proterozoic anorthosite. Contributions to Mineralogy and Petrology 119, 166–180.

Mitchell, J.N., Scoates, J.S., Frost, C.D., Kolker, A., 1996a. The geochemical evolution of anorthosite residual magmas in the Laramie anorthosite complex, Wyoming. Journal of Petrology 37, 637–660.

Mitchell, R.H., Eby, G.N., Martin, R.F. (Eds.), 1996b. Alkaline Rocks: Petrology and Mineralogy. Canadian Mineralogist, vol. 34, pp. 175–484.

Mitchell, R.H., Platt, R.G., 1982. Mineralogy and petrology of nepheline syenites from the Coldwell alkaline complex, Ontario, Canada. Journal of Petrology 23, 186–214.

Morogan, V., Upton, B.G.J., Fitton, J.G., 2000. The petrology of the Ditrau alkaline complex, Eastern Carpathians. Mineralogy and Petrology 69, 227–265.

Morse, S.A., 1981. Kiglapait geochemistry: IV. The major elements. Geochimica et Cosmochimica Acta 45, 461–479.

Nekvasil, H., Dondolini, A., Horn, J., Filiberto, J., Long, H., Lindsley, D.H., 2001. The origin and evolution of silica-saturated alkalic suites: an experimental study. Journal of Petrology 45, 693–721.

O'Brien, H.E., Irving, A.J., McCallum, I.S., Thirlwall, M.F., 1995. Strontium, neodymium, and lead isotopic evidence for the interaction of post-subduction asthenospheric potassic mafic magmas of the Highwood Mountains, Montana, USA, with ancient Wyoming craton lithospheric mantle. Geochimica et Cosmochimica Acta 59, 4539–4556.

Olson, K.E., 1992. The petrology and geochemistry of mafic igneous rocks in the anorthosite-bearing Adirondack Highlands, New York. Journal of Petrology 33, 471–502.

Panter, K.S., Kyle, P.R., Smellie, J.L., 1997. Petrogenesis of a phonolite–trachyte succession at Mount Sidley, Marie Byrd Land, Antarctica. Journal of Petrology 38, 1225–1253.

Parrish, R.R., 1987. An improved micro-capsule for zircon dissolution in U–Pb geochronology. Isotope Geoscience 66, 99–102.

Paul, D.K., Ray Barman, T., McNaughton, N.J., Flecther, I.R., Potts, P. J., Ramakrishnan, M., Augustine, P.F., 1990. Archaean–Proterozoic evolution of Indian charnockites: isotopic and geochemical evidence from granulites of the Eastern Ghats belt. Journal of Geology 98, 253–263.

Pearce, J.A., Harris, N.W., Tindle, A.G., 1984. Trace element discrimination diagrams for the tectonic interpretation of granitic rocks. Journal of Petrology 25, 956–983.

Phillips, G.N., Wall, V.J., Clemens, J.D., 1981. Petrology of the Strathbogie batholith: a cordierite-bearing granite. Canadian Mineralogist 19, 47–63.

Potter, L.S., 1996. Chemical variation along strike in feldspathoidal rocks of the eastern alkalic belt, Trans-Pecos Magmatic Province, Texas and New Mexico. Canadian Mineralogist 34, 241–264.

Powell, M., 1978. The crystallization history of the Igdlerfigssalik nepheline syenite intrusion, Greenland. Lithos 11, 99–120.

Powell, M., Powell, R., 1977. A nepheline–alkali feldspar geothermometer. Contributions to Mineralogy and Petrology 62, 193–204.

Price, R.C., Johnson, R.W., Gray, C.M., Frey, F.A., 1985. Geochemistry of phonolites and trachytes from the summit region of Mount Kenya. Contributions to Mineralogy and Petrology 89, 394–409.

Ramakrishnan, M., Nanda, J.K., Augustine, P.F., 1998. Geological evolution of the Proterozoic Eastern Ghats Mobile Belt. Geological Survey of India Special Publication 44, 1–21.

Rao, A.D.P., Rao, K.N., Murty, Y.G.K., 1987. Gabbro–anorthosite–pyroxenite complexes and alkaline rocks of Chimakurti–Elchuru area, Prakasam District, Andhra Pradesh. Records of Geological Survey of India 116, 1–20.

Rao, A.T., Satyanarayana, P.V.V., Yoshida, M., 1998. Geothermometry of coexisting pyroxenes from Chimakurti Anorthosite Complex at the contact of Eastern Ghats Granulite and Nellore Granite–Greenstone Belts, Andhra Pradesh, India. Gondwana Research Group Memoir 4, 165–184.

Ratnakar, J., Leelanandam, C., 1989. Petrology of the alkaline plutons from the eastern and southern Peninsular India. In: Leelanandam, C. (Ed.), Alkaline Rocks. Memoir Geological Society of India, vol. 15, pp. 145–176.

Ratnakar, J., Vijaya Kumar, K., 1995. Petrogenesis of quartz-bearing syenite occurring within nepheline syenite of the Elchuru alkaline complex, Prakasam Province, Andhra Pradesh. Journal of the Geological Society of India 46, 611–618.

Rickers, K., Mezger, K., Raith, M.M., 2001. Evolution of the continental crust in the Proterozoic Eastern Ghats Belt, India and new constraints for Rodinia reconstruction: implications from Sm–Nd, Rb–Sr and Pb–Pb isotopes. Precambrian Research 112, 183–210.

Rock, N.M.S., 1978. Petrology and petrogenesis of the Monchique alkaline complex, Southern Portugal. Journal of Petrology 19, 171–214.

Royse, K.R., Noble, S.R., Tarney, J., Cadman, A.C., 1999. Country-rock contamination of marginal mafic granulites bordering the Nain plutonic suite: implications for mobilization of Sr during high-grade contact metamorphism. Canadian Journal of Earth Sciences 36, 985–997.

Sarkar, A., Paul, D.K., 1998. Geochronology of the Eastern Ghats Precambrian Mobile Belt – a review. Geological Survey of India Special Publication 44, 51–86.

Sarkar, A., Nanda, J.K., Paul, D.K., Bishui, P.K., Gupta, S.N., 1989. Late Proterozoic alkaline magmatism in the Eastern Ghats Belt: Rb–Sr isotopic study on Koraput complex, Orissa. Indian Minerals 43, 23–29.

Scoates, J.S., Mitchell, J.N., 2000. The evolution of troctolitic and high Al basaltic magmas in Proterozoic anorthosite plutonic suites and implications for the Voisey's Bay massive Ni–Cu sulfide deposit. Economic Geology 95, 677–701.

Scoates, J.S., Frost, C.D., Mitchell, J., Lindsley, D.H., Frost, B.R., 1996. Residual-liquid origin for a monzonitic intrusion in a mid-Proterozoic anorthosite complex: the Sybille intrusion, Laramie anorthosite complex, Wyoming. Geological Society of America Bulletin 108, 1357–1371.

Shaw, R.K., Arima, M., Kagami, H., Fanning, C.M., Shiraishi, K., Motoyoshi, Y., 1997. Proterozoic events in the Eastern Ghats Belt, India: evidence from Rb–Sr, Sm–Nd systematics, and SHRIMP dating. Journal of Geology 105, 645–656.

Smith, D.R., Noblett, J., Wobus, R.A., Unruh, D.M., Chamberlain, K.R., 1999a. A review of the Pikes Peak batholith, Front Range, central Colorado: a "type example" of A-type granitic magmatism. Rocky Mountain Geology 34, 289–312.

Smith, D.R., Noblett, J., Wobus, R.A., Unruh, D.M., Douglass, J., Beane, R., Davis, C., Goldman, S., Kay, G., Gustavson, B., Saltoun, B., Stewart, J., 1999b. Petrology and geochemistry of late-stage intrusions of the A-type, mid-Proterozoic Pikes Peak batholith (central Colorado, USA): implications for petrogenetic models. Precambrian Research 98, 271–305.

Sørenson, H. (Ed.), 1974. The Alkaline Rocks. John Wiley, New York.

Speer, J.A., 1981. Petrology of cordierite- and almandine-bearing granitoid plutons of the southern Appalachian Piedmont, U.S.A. Canadian Mineralogist 19, 35–46.

Stacey, J.S., Kramers, J.D., 1975. Approximation of terrestrial lead isotope evolution by a two-stage model. Earth and Planetary Science Letters 26, 207–221.

Steiger, R.H., Jäger, E., 1977. Subcommission on geochronology: convention on the use of decay constants in geo- and cosmochemistry. Earth and Planetary Science Letters 36, 359–362.

Sun, S.-s., McDonough, W.F., 1989. Chemical and isotopic systematics of oceanic basalts: implications for mantle composition and processes. In: Saunders, A.D., Norry, M.J. (Eds.), Magmatism in the Ocean Basins. Geological Society Special Publication, vol. 42, pp. 313–345.

Thomas, M.D., 1990. Deep structure of Middle Proterozoic anorthositic intrusions in the eastern Canadian Shield: insights from gravity modelling. In: Gower, C.F., Rivers, T., Ryan, B. (Eds.), Mid-Proterozoic Laurentia–Baltica. Geological Association of Canada Special Paper, vol. 38, pp. 353–372.

Thomson, R.N., Fowler, M.B., 1986. Subduction-related shoshonitic and ultrapotassic magmatism: a study of Siluro-Ordovician syenites from the Scottish Caledonides. Contributions to Mineralogy and Petrology 94, 507–522.

Thomson, R.N., Leat, P.T., Dickin, A.P., Morrison, M.A., Hendry, G.L., Gibson, S.A., 1990. Strongly potassic mafic magmas from lithospheric mantle sources during continental extension and heating: evidence from Miocene minettes of northwest Colorado, U.S.A. Earth and Planetary Science Letters 98, 139–153.

Upadhyay, D., Raith, M.M., 2006. Petrogenesis of the Kunavaram alkaline complex and the tectonothermal evolution of the neighboring Eastern Ghats Belt granulites, SE India. Precambrian Research. 2006. doi:10.1016/j.precamres.2006.07.006.

Upadhyay, D., Raith, M.M., Mezger, K., Hammerschmidt, K., 2006. Mesoproterozoic rift-related alkaline magmatism at Elchuru, Prakasam Alkaline Province, SE India. Lithos 89, 447–477.

Vijaya Kumar, K., Ratnakar, J., 1999. Mineral chemistry and genesis of phlogopites from the gabbros of Ravipadu, Prakasam province, Andhra Pradesh, India. Journal of the Geological Society of India 53, 39–48.

Vijaya Kumar, K., Ratnakar, J., 2001. Petrogenesis of the Ravipadu gabbro pluton, Prakasam province, Andhra Pradesh. Journal of the Geological Society of India 57, 113–140.

Weis, D., Frey, F.A., Leyrit, H., Gautier, I., 1993. Kerguelen Archipelago revisited: geochemical and isotopic study of the Southeast Province lavas. Earth and Planetary Science Letters 118, 101–119.

Wittke, J.H., Mack, L.E., 1993. OIB-like mantle source for continental alkaline rocks of the Balcones Province, Texas: trace-element and isotopic evidence. Journal of Geology 101, 333–344.

Woolley, A.R., Platt, R.G., 1986. The mineralogy of nepheline syenite complexes from the northern part of the Chilwa Province, Malawi. Mineralogical Magazine 50, 597–610.

Zartman, R.E., Doe, B.R., 1981. Plumbotectonics – the model. Tectonophysics 75, 135–162.

Zozulya, D.R., Bayanova, T.B., Eby, G.N., 2005. Geology and age of the Late Archean Keivy alkaline province, Northeastern Baltic Shield. Journal of Geology 113, 601–608.